Review

Optical Fiber Based Temperature Sensors: A Review

Rahul Kumar Gangawar , Sneha Kumari * , Akhilesh Kumar Pathak * , Sai Dheeraj Gutlapalli , Mahesh Chand Meena

Posted Date: 10 February 2023

doi: 10.20944/preprints202302.0180.v1

Keywords: Waveguide; photonic crystal; optical fiber; Bragg gratings; temperature; sensor; COVID

Review

Optical Fiber Based Temperature Sensors: A Review

Rahul Kumar Gangwar [1], Sneha Kumari [2,*], Akhilesh Kumar Pathak [3,*], Sai Dheeraj Gutlapalli [4] and Mahesh Chand Meena [1]

[1] Department of Physics & Electronics, Rajdhani College, University of Delhi, New Delhi, 110015, India
[2] Centre for Nanoscience and Engineering (CeNSE), Indian Institute of Science, Bengaluru, 560012, India
[3] Center for Smart Structures and Materials, Department of Mechanical Engineering, Northwestern University, Evanston, IL, 60208, USA
[4] Richmond University Medical Center affiliated with Mount Sinai Health System and Icahn School of Medicine, Staten Island, New York, 10310, USA
* Correspondence: akhilesh.pathak@northwestern.edu (S.K.); snehakumari@iisc.ac.in (A.K.P.)

Abstract: Current generation witnesses a huge interest in optical waveguide due to their salient feature such as low cost, immune to electromagnetic interference, easy to multiplex, compact size, etc. These features of the optical fibers makes it an useful tool for various sensing applications including medicine, automotive, biotechnology, food quality control, aerospace, physical and chemical monitoring etc. Among all the reported application, the device has been widely exploited to measure the physical and chemical variation in surrounding environment. Optical fiber based temperature sensor plays a crucial role in this decade to detect high fever and tackle COVID like pandemic. Recognizing the major developments in the field of the optical fibers, this article aims to provide recent progress in temperature sensor utilizing several sensing configuration including standard fiber, photonic crystal fiber, and Bragg grating fibers. Additionally, the article also highlights the advantages, limitations, and future possibilities in this area.

Keywords: Waveguide; photonic crystal; optical fiber; Bragg gratings; temperature; sensor; COVID

1. Introduction

The reliable temperature monitoring plays a key role in the metallurgical industry, aerospace field, nuclear energy production, and medical applications [1,2]. In the metallurgical industry, a real-time monitoring of the internal temperature of high-temperature boilers is keys to measure combustion efficiency and the safety prevention [3,4]. On other hand, temperature monitoring inside the turbines and combustion chambers of an aero-engine or aircraft can help extending its service life [5–7]. Recently, the appearance of COVID-19 gain huge interest in temperature monitoring instruments in medical sector for continuous monitoring temperature of individuals at public places [8,9]. Extremely harsh environments with high pressures, high temperatures, and strong electromagnetic radiation present a challenge to convectional temperature sensors.

According to the accuracy, detection and installation techniques, high-temperature monitoring technology can be categorized in two categories (i) contact measurement [10], and (ii) non-contact measurement [11]. Thermocouple sensors made of expensive metals are generally utilized for former type of temperature sensing due to their ease of operation, mature preparation approach, and wide operating range [12]. However, the thermocouple sensors suffer several limitations such as short life, poor corrosion resistance, low accuracy, and susceptibility to electromagnetic interferences. The main concerns of thermocouple devices are its metal or alloys used during the fabrication can be easily oxidized and damaged at high temperatures leading to a shorter service life and sensing accuracy [13]. Infrared thermography is a type of non-contact temperature sensing technology, which is designed to avoid direct contact between the sensing equipment and high-temperature environment to provide a non-destructive sensing performance [14]. Unfortunately, the radiation temperature monitoring technology is suitable only for the surface measurements, i.e., explosion flame, and cannot detect the temperature of the internal structure of the closure device.

Preprints (www.preprints.org) | NOT PEER-REVIEWED | Posted: 10 February 2023 doi:10.20944/preprints202302.0180.v1

Compared to conventional sensing technology, optical fiber based sensors have gain huge interest owing to their excellent properties such as low cost, compact size, able to multiplexing and immune to electromagnetic interferences [15]. Till date, several approach have already been implemented for temperature sensing including photonic crystal fiber (PCF) [16], standard fiber (such as single-mode fiber (SMF) and multi-mode fiber (MMF)) [17], grating based fibers (e.g., fiber Bragg grating (FBG), long period grating (LPG), and tilted FBG (TFBG)) [18]. The commonly employed high-temperature sensing optical fibers are mainly includes silica and crystal fibers. Theoretically, the maximum temperature which a temperature sensor can detect based on the fiber materials rather than that of it's the sensing mechanism. Usually, the silica-fiber-based temperature sensors are limited to operating within 1000 °C due to the diffusion of germanium dopant [1]. Additionally, temperature sensors based on pure silicon fibers such as PCF and microstructure fiber can operate at 1300 °C which is closer to the melting point of silicon, whereas, the temperature sensors based on single-crystal fibers can operate stably below 1900 °C. Figure 1 illustrates the summary of all types of optical fiber temperature sensors.

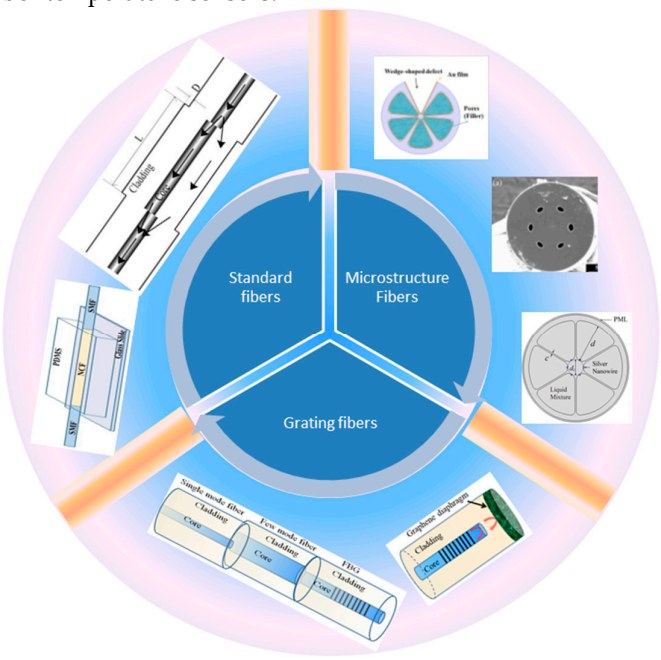

Figure 1. Summary of various optical fiber based temperature sensors**.**

In this article we have reviewed several optical fiber based temperature sensors reported in past decades, including their design, fabrication, sensing materials, and performance. This review is organized in following manner: Section 2 provide a brief survey over microstructure optical fiber along with the advancement in the technology; section 3 cover the standard single mode fiber (SMF) and multi-mode fibers (MMF) and their application in temperature sensing; section 4 comprises grating based fibers and their role in temperature sensing. Finally, section 5 provides the brief on future prospects and challenges. Finally the overall conclusion is drawn in section 6.

2. Microstructure optical fiber (MOF):

The last decade has shown the enormous interest in optical fibers used for sensing and long-distance operation applications. The optical fiber in sensors applied as a sensing element to monitor surrounding parameters like strain, pressure, vibration, temperature, etc. . Numerous types of fiber-optic temperature sensors, including as Microstructured Fiber, fibre Bragg gratings (FBGs), long-period gratings (LPGs), Rayleigh scattering, Brillouin scattering, and Raman scattering, have been created for the purpose of monitoring the health of social infrastructures and industrial equipment [19–24]. Unlike standard optical fibres, photonic crystal fibres (PCFs) are made up of small air holes

Preprints (www.preprints.org) | NOT PEER-REVIEWED | Posted: 10 February 2023 doi:10.20944/preprints202302.0180.v1

that are spaced at regular intervals, allowing for greater design freedom and unique optical properties [25,26]. Based on post-processing techniques, the micro air holes can also be filled with liquid, gas, or even solid materials, greatly changing the PCF guiding characteristics and allowing the fabrication of a variety of functional fibre devices such as electrically controlled optical switches [27–29], all-optical modulators [30], temperature-controlled tunable optical filters [31] photonic bandgap fibre polarimeters [32,33], and PCF sensors [34]. In this section, the current status of research on microstructured fiber based temperature sensors is discussed.

Micro optical devices have been quickly developed in recent years as a result of technological advancements in micro-fiber manufacturing [35,36], particularly in the field of dynamic temperature monitoring [37]. A number of significant efforts have been made to improve the sensitivity and reliability of the proposed optical fiber-based temperature sensors, including micron scale processing of couplers and ring resonators [38,39], selective liquid infiltration of high birefringence photonic crystal fibres (HBPCFs) [40,41] and filled photonic crystal fibres [42,43]. Most temperature sensors based on classic fibre constructions with silica backgrounds have temperature sensitivity less than 0.3 nm/°C [44], which is primarily constrained by the modest thermo-optical coefficient difference between the fibre core and cladding. To circumvent these constraints, Qian et al suggested a photonic crystal fibre (PCF)-based temperature sensor that reached an extrahigh sensitivity of 6.6 nm/°C by selectively infiltrating a thermosensitive liquid, such as alcohol, in the air holes to increase the thermo-optic coefficient [45]. In this experiment, the fiber loop mirror of alcohol filled highly birefringence PCF is placed in a temperature controlled container for investigating the temperature characteristics of the proposed sensing device. Figure 2 shows the experimental setup for the temperature measurement and inset of the Figure 2 shows the cross section of the highly birefringence PCF. Dora et al [28,46] suggested a temperature sensitive device based on nematic liquid crystal filled photonic crystal fibre, with a temperature sensitivity of 3.90 nm/°C.

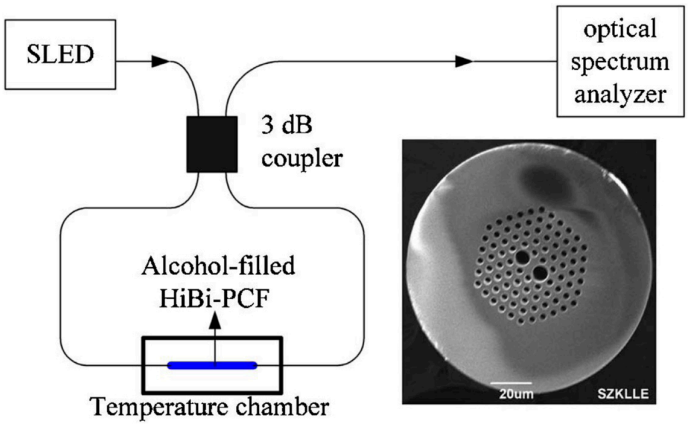

Figure 2. Experimental setup for a temperature sensor based on an FLM. Inset: SEM of the used HiBi-PCF [45].

Due to its strong thermal resistance and immunity to electromagnetic noise and corrosion, fibre sensors are likely the only option for sensing at temperatures above 800 °C. In 2013, Chen et al. described for the first time a true distributed pressure sensing at room and very high temperature sensing by utilising a pressure-sensitive fibres. It is based on an optical frequency domain reflectometry measurement of Rayleigh scattering in a fibre. This technique has been used to provide a distributed sensing solution for measurements of temperature, axial strain, and transverse stress. Air-hole microstructural fibres are employed to broaden its applicability for pressure sensing at high temperatures. Temperatures ranging from 24 °C to 800 °C are used to detect pressure distributions of up to 13.8 MPa (2000 psi) [47]. Another method for measuring temperature is to utilise Fabry-Pérot interferometers (FPI). Because of its sensitivity, extremely tiny size, easy design, and versatility in modifying sensitivity and dynamic range, FP interferometers are a common sensor arrangement. A microstructure temperature sensor that can be wavelength and frequency encoded at the same time

Preprints (www.preprints.org) | NOT PEER-REVIEWED | Posted: 10 February 2023 doi:10.20944/preprints202302.0180.v1

presented by the Li et al. [48]. In this work, the sensor system has the potential for over 1000 multiplexing capacity via a single fibre with the hybrid frequency-division-multiplexing/wavelength-division-multiplexing (FDM/WDM) method. The temperature sensitivity of roughly 7.91 pm/°C is established experimentally using quasi-distributed measurement of temperature change. Tan et al. presented a work which shows how to make an intrinsic FPI sensor for high temperature detection with high fringe contrast by splicing a short piece of microstructured fibre to an single mode fiber [49]. The two strands of the microstructured fiber are spliced together using the conventional arc-discharge process. The interference spectrum's fringe contrast can approach 20 dB. There is theoretical study and thermal testing up to 1000°C. Monitoring the dip wavelength shift yields a temperature sensitivity of 17.7 pm/°C. This suggested sensor is small and has a significant potential for high temperature sensing applications using simply splicing and cleaving techniques.

To metallize a fibre surface in a typical fiber-based sensor, first strip the fibre jacket and then physically or chemically remove the fibre cladding, nearly to the core, to permit evanescent coupling with a plasmon mode. The associated operations directly raise the overall fabrication cost and jeopardise device dependability. The rapid creation of a novel form of PCF with an array of air holes along the propagation direction has piqued the curiosity of researchers worldwide in recent years. Many studies sought to insert metallic layers or rods into PCF and were successful in containing the plasmonic modes within the fibre [50–52]. Metallization of PCFs can be accomplished using stack-and-draw [53] or by pumping molten metal into the hollow channels of silica glass PCFs [52]. Metal layers can be deposited in the side of the PCF using either a high pressure chemical vapour deposition (CVD) approach [53] or a wet chemistry deposition process employed in the manufacture of metal-covered hollow waveguides [54]. In 2013, Favero et al experimentally demonstrate a PCF with a specially doped germanium core as shown in Figure 3a [55]. PCF with germanium core sandwiched between two single mode fibers to form an interferometer for the temperature measurement. The experimental set for the temperature detection is shown in Figure 3b. One end of the fiber was deposited with the gold film in order to work in the reflection mode. Proposed device shows very high temperature dependence with the sensitivity of 78 pm/°C.

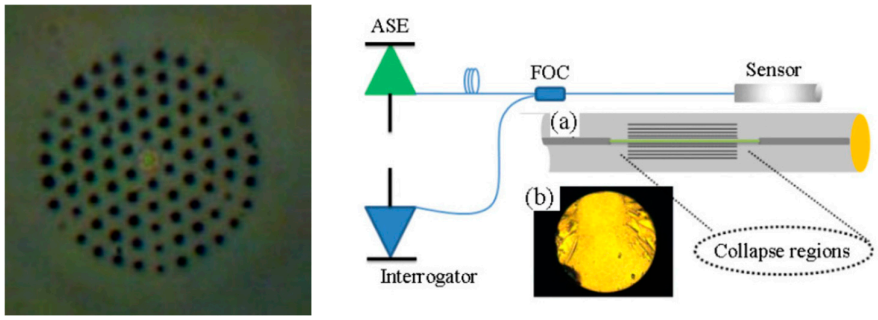

(**a**) (**b**)

Figure 3. (a) Cross section of the Microstructure fiber and, (b) experimental setup with collapsed region of the microstructure fiber and gold coated at the one end of the single mode fiber [55].

By inserting a silver nanowire into the holes of a six hole PCF, a temperature sensor was designed based on the surface plasmon resonance effect [56]. Cross sectional area of the proposed sensing device is shown in Figure 4a and different air holes coated with silver nanowires and filled with the high thermos-optic coefficient liquid, a mixture of ethanol and chloroform is shown in Figure 4b. As a sensing medium, a liquid combination (ethanol and chloroform) with a high thermo-optic coefficient is injected into the PCF holes. The filled silver nanowires can sustain resonance peaks, and the peak will move when temperature changes cause changes in the mixture's refractive indices. The temperature change may be observed by monitoring the peak shift. Because the refractive index of the filled mixture is near to that of the PCF material, the resonance peak is particularly temperature sensitive. Our numerical results show that a temperature sensitivity of up to 4 nm/K is possible.

Preprints (www.preprints.org) | NOT PEER-REVIEWED | Posted: 10 February 2023 doi:10.20944/preprints202302.0180.v1

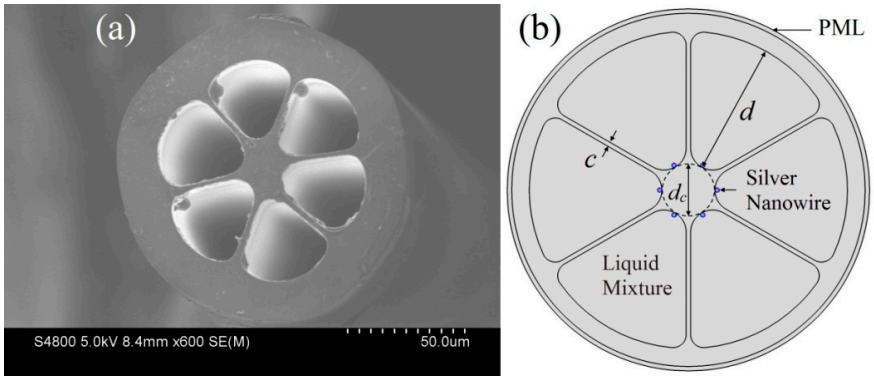

Figure 4. (**a**) Cross-section of the six-hole PCF; (**b**) Schematic of the proposed sensing device coated with silver nano wires and filled with the mixture of ethanol and chloroform [56].

A sensing device with improve sensitivity based on the microstructured optical fiber and worked on the surface plasmon resonance principle was further demonstrated by the same group in 2014 [57]. The MOF's air holes are coated with a silver metal and filled with mixture of ethanol and chloroform which have a very high thermo-optic coefficient. The usage of all six fibre openings, as well as their relatively large size, should make silver coating and liquid mixture filling easier. Temperature fluctuations will cause changes in the coupling efficiency between the core-guided mode and the plasmonic mode, resulting in various loss spectra being recorded. The liquid mixture's refractive index is near to that of the MOF material, which improves coupling efficiency and sensitivity. Numerical results depict the temperature sensitivity of 5.6 nm/K and that the most sensitive range of the sensor can be modified by varying the volume ratios of ethanol and chloroform. Apart from these structures, different temperature sensing devices with different configuration of the MOF are demonstrated [58–61]. In 2015, Scarcia et al. conducts an accurate theoretical analysis of the viability of a unique fibre optic temperature sensor designed as a standalone device. It is built on a trio of integrated/spliced microstructured optical fibres (MOFs). The first incorporates an appropriate cascade of LPGs into the core. The other two sensor parts are a single mode intermediate MOF and a ytterbium doped MOF laser. The three MOFs are made to be readily spliced together as shown in Figure 5. The entire design is carried out using ad hoc computer code created specifically for this purpose. A low-cost pump diode laser at 980 nm wavelength and a commercial optical power detector are all that is required for a comprehensive temperature monitoring setup. The simulated sensitivity S = 315.1 μW/°C and operation range ΔT = 100°C are adequate for real-world applications [62]. In [63], two all-fiber loop mirrors employing a clover microstructured fibre for simultaneous temperature and strain monitoring are demonstrated. The design of the fibre allowed for the observation of various interferences caused by the microstructured fibre core section. Different sensitivity to temperature and strain were obtained, and both physical characteristics may be discriminated using a matrix technique. For temperature and strain, resolutions of ±2 °C and ±11 με for the first structure and ±2.3 °C and ±18 με for the second were obtained.

Preprints (www.preprints.org) | NOT PEER-REVIEWED | Posted: 10 February 2023 doi:10.20944/preprints202302.0180.v1

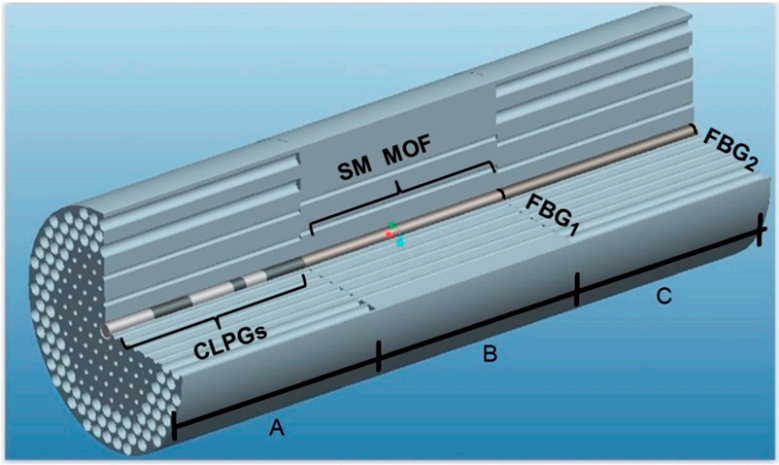

Figure 5. Cross section of the proposed temperature sensor [62].

A wide variety of the MOF based temperature sensors has been developed by using the different configuration and sensing techniques [64–70]. In [71], use of femtosecond laser ablation to etch fibre Bragg gratings into the core of pure silica suspended-core microstructured optical fibre (SCFs) is presented. Because the concentrated femtosecond laser beam is not greatly deformed when travelling through the fibre cladding, the SCF's basic shape (three big holes) enables for direct writing of FBGs. These can withstand temperatures of up to 1300°C and can be wavelength divided multiplexed. Temperature sensing up to 1100°C was achieved by measuring the interference spectrum's fringe changes as temperature varied [72]. The sensor head in this study is constructed by splicing a single mode fibre (SMF) with a suspended core microstructured optical fiber (SCF), resulting in an SMF-2SCF-SMF configuration since the reflected light travels twice the physical length of the SCF. Because the SCF is a single-material device, extremely high temperatures may be measured, while the sensor head's all-splice simplicity results in low-cost and steady operation.

In [73], a very sensitive temperature sensor based on an all-fiber Sagnac loop interferometer and metal-filled side-hole PCF demonstrated. PCFs with two side holes filled with metal provide a structure that may be adjusted to modify the birefringence of the fibre by expanding the filler metal. To investigate the influence of filler metal on the temperature sensitivity of the fiber-optic temperature sensor, bismuth and indium were utilised. Measurements revealed that the indium-filled side-hole PCF could obtain a very high temperature sensitivity of 9.0 nm/°C. An unique microstructure fibre based on side-polished fibre (SPF) presented in [74] for the temperature sensing application. Polystyrene microspheres were self-assembled onto the side-polished surface of SPF to generate the microstructure fiber's colloidal crystal coating. Three primary troughs were identified in the transmission spectrum due to the Bragg reflection of the colloidal crystals coating and the strong interaction between evanescent field and colloidal crystal. The valley modulation amplitude might reach 12 dB. Furthermore, the transmission valley demonstrated strong temperature sensitivity. Transmission optical power exhibited temperature sensitivity was up to 0.487 dB/°C. A brief description about the different sensing structure and mechanism also reported in [75].

By using the optimal polymer optical fiber for Bragg grating sensing, fabrication and analysis of an infinitely single mode microstructured polymer optical fiber presented in [76]. This fibre is constructed of cyclo-olefin homopolymer Zeonex grade 480R, which has a very high glass transition temperature of 138 °C and is not affected by humidity. The temperature sensitivity of this fiber is 24.01 ± 0.1 pm/°C for both increasing and decreasing temperature. Apart from these sensing devices for temperature measurement, many researcher used MOF for the simultaneously measurements of the two or more physical parameters [77–79]. In [80], a linearly chirped bragg grating fibre engraved in a microstructured polymer optical fibre used for the temperature detection during thermal treatments. A KrF laser and uniform phase mask were used to inscribe a CFBG of 10-mm length and 0.98-nm bandwidth in a mPOF fibre. The temperature sensitivity of the CFBG is 191.4 pm/°C. A novel

Preprints (www.preprints.org) | NOT PEER-REVIEWED | Posted: 10 February 2023 doi:10.20944/preprints202302.0180.v1

sensing approach based on C-type micro-structured fibre for simultaneous monitoring of seawater temperature and salinity was presented by Zhao et al. [81]. The C-type fibre structure as shown in Figure 6, was created by removing the outer wall of one pore from a six-hole micro-structured fibre, allowing birefringence to enter and breaking the original pattern of degeneracy. Furthermore, a gold layer was applied to the structure's surface to improve sensing sensitivity using the SPR phenomena. Model studies demonstrated that the suggested filling structure might generate two SPR loss valleys with distinct sensitivity to temperature and salinity. Maximum temperature sensitivity of 7.609 nm/°C was obtained for Y polarisation, demonstrating that the designed scheme could not only solve the cross sensitivity problem of two parameters but also achieve high sensitivity.

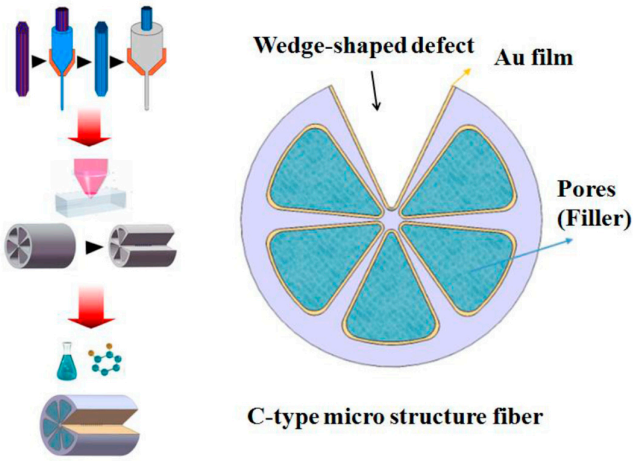

Figure 6. Cross section of the proposed temperature sensing device [81].

In recent year, using of microstructure optical fiber in sensing filed with different configuration earned a lot of attention [82–84]. In [85], Su et al. proposed a high temperature sensor which is based on the suspended –core microstructure optical fiber (SCMF). The sensor is fabricated by fusing a portion of SCMF between two portions of the multimode fiber (MMF). This kind of configuration made multimode interference by the air cladding modes and the core modes in the SCMF. The transmission spectra of the MMF-SCMF-MMF structure are filtered using the Fast Fourier transform. The wavelength shift of the main spatial frequency is measured when the temperature varies between 50 and 800 degrees Celsius. Sensitivities of 31.6 pm/°C and 51.6 pm/°C are reached in the temperature ranges of 50°C - 450°C and 450°C - 800°C, respectively. By using the Fabry-Perot interferometer, Zhao et al. [86] proposed and experimentally demonstrated composite cavity fiber tip for high temperature sensing. An air cavity and a silica cavity make up the composite cavity. An oval air hole inserted in the SMF serves as the air cavity. A small segment of SMF cascaded to the air cavity forms the silica cavity. The CCFT was effectively encased by a tapered-shaped silica capillary to eliminate the effects of other external physical characteristics (refractive index, humidity, etc.) on the CCFT FPI. The packed CCFT FPIs were used for high temperature sensing in the 100-800 °C range. The silica cavity has a temperature sensitivity of 14.31 pm/°C.

The finite element approach was used to examine a temperature sensor based on a Sagnac interferometer and a liquid crystal-filled microstructured optical fibre [87]. Near the core of the fiber, six submicron liquid crystal columns were added whose refractive index in slightly greater than the silica. In this configuration, the power of the fundamental core modes remained restricted to the silica core, and the mode field properties were heavily impacted by the six submicron liquid crystal columns. The temperature-sensing property of the resultant liquid crystal-filled microstructured optical fibre in the range of 265-325 K was examined using a Sagnac interferometer based on the thermo-optic effect. The temperature sensitivity was 6.23 nm/K with high linearity in the region of 265-295 K. Zhao et al. demonstrated a Sagnac interferometer temperature sensor based on the

glycerine filled MOF [88]. Here, the photosensitive substance was a glycerin solution which is filled in a polarization-maintaining photonic crystal fibre (PMPCF). According to the finite element approach, the temperature sensor had the maximum sensitivity when the PMPCF was filled with a 70% mass fraction of glycerine solution. A linear fit was built between the dip wavelength and the temperature in the experiment, with the temperature rising from -25 °C to 85 °C in 5 °C steps. The findings showed that the suggested sensor had the greatest temperature sensitivity of 1.5005 nm/°C within the temperature range of -25 °C to 85 °C.

In another work, the finite element approach has suggested a very sensitive temperature sensor for magnetic fluid (ethanol) utilising a ring-core-based microstructured optical fibre (MOF) with two huge elliptical air holes alongside the ring core [89]. To boost the ring core's high sensitivity responsiveness, highly sensitive magnetic fluid ethanol is introduced. For the broad working wavelength range of 6500-7000 nm and temperature range of 10-60°C and applied magnetic field strength range of 50-200 Oe, the highest sensitivity response of 25,641.025 nm/RIU and 10 nm/°C is achieved. Here, the sensing device simultaneously measured three different physical parameters. In [90], an investigated was carried out for a temperature sensor based on the modes coupling effect in a liquid crystal-filled MOF. A full-vectorial finite-element technique (FEM) with completely matched layer and scattering boundary conditions was used to study the sensing properties. Liquid crystal E7 was developed to be infiltrated into one cladding air hole in PCF to generate a defect core for temperature sensing. As the phase matching requirement is met, the core modes couple to a variety of ordered defect core modes, resulting in a significant rise in the confinement loss spectrum. In an approach, [91] experimentally demonstrated a temperature sensor based on the Yb-doped silica micro-structured optical fibers. In this work, authors describe an unique method for producing Yb-doped silica microstructured optical fibres and its application in high-temperature optical fibre sensing. The Yb-doped silica micro structured optical fibre preforms were made out of Yb-doped silica core rods (0.1 wt% Yb2O3) and holey pure silica claddings created using UV curable tube moulding and digital light processing 3D printing techniques, respectively. The rod-in-tube approach was used to draw silica preforms to Yb-doped silica microstructured optical fibres without causing significant deformation. Doped microstructured fibres were used in high-temperature sensing ranging from 296.15 to 653.15 K. Figure 7a depicts the scanning microscopic image of the fabricated Yb-doped silica microstructured optical fibres and the refractive index profile of this MOF is shown in Figure 7b–d depicts the attenuation spectrum and absorption loss of the proposed MOF based sensing device. The experimental results shows that the proposed sensing device have maximum value of temperature sensitivity and relative temperature sensitivity of 0.0023 K at 348 K and 0.8%/K at 296K respectively.

Preprints (www.preprints.org) | NOT PEER-REVIEWED | Posted: 10 February 2023 doi:10.20944/preprints202302.0180.v1

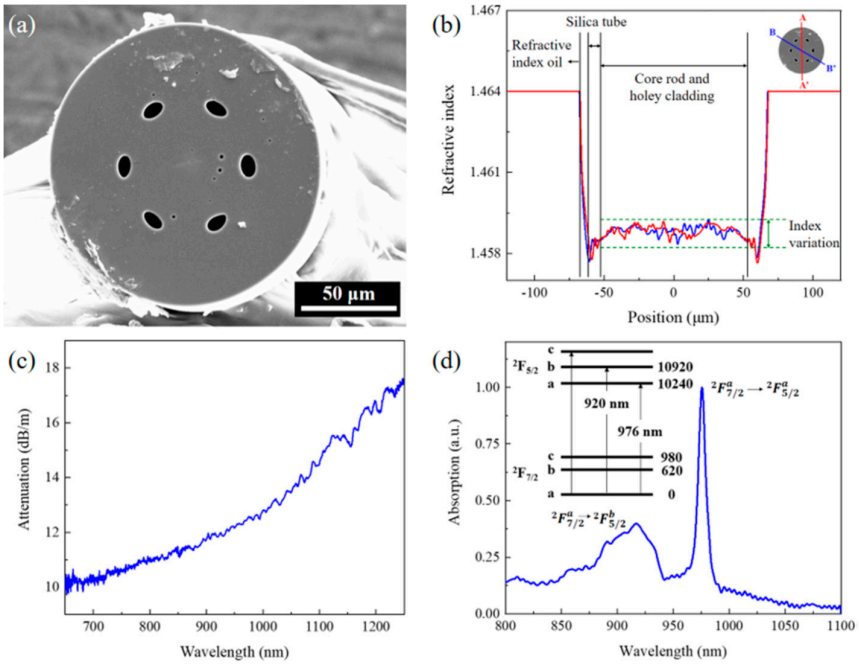

Figure 7. (a) SEM image of the Yb-doped silica micro-structured optical fiber, (b) Refractive index profile of the fabricated Yb-doped silica micro-structured optical fiber along different directions, (c) variation of attenuation of the fiber with different wavelenght, and (d) absorption spectrum of the fiber [91].

Theoretical analyses represent a temperature sensor with a high sensitivity based on the MOF Sagnac interferometer [92]. Ethanol is inserted in the air holes of the MOF. Two big air holes are also introduced for enhancing the birefringence and sensitivity of the proposed device. Simulation results shows that the proposed MOF temperature sensor has sensitivity of 14.7 nm/°C in the temperature range varies from 15 to 75 °C. In [93], the silver mirror reaction was used for coating the silver film on the surface of self-made MOF to stimulate the surface plasmon resonance effect, and Polydimethylsiloxane (PDMS) with a high thermal-optical coefficient was coated on the silver film as temperature-sensitive material. The MOF with silver and PDMS films was coupled with multi-mode fiber on both sides to form the temperature sensor. In this sensor system, the energy is coupled into the cladding of the microstructure fiber by multi-mode fiber, and the surface plasmon resonance can be further excited in the MSF. The refractive index of PDMS changes with change in the temperature of the external environment. The proposed sensors exhibits very high sensitivity of 0.83 nm/°C and -0.84 nm/°C during heating and cooling for the temperature range of 35 °C to 95 °C, respectively.

Apart from these sensing techniques, researcher used nonlinear properties of the MOF for the sensing purpose. A unique fiber-optic soliton self-frequency shift (SSFS) temperature sensor was developed, which was built utilising an in-house MOF [94]. SSFS-based sensing was systematically examined using this sensor with variations in average pump wavelength and pump power. The sensing performance of the proposed sensor was assessed experimentally and conceptually, subject to the average pump wavelength and pumps power, by detecting the centre wavelength shift of the 3-dB bandwidth of the soliton with temperature change. Greater sensitivity was achieved when the pump wavelength is longer while the average pump power was fixed. At an average pump power of 300 mW and pump wavelength of 1600 nm, the maximum sensitivity of the proposed sensing device comes to be 1.759 nm/°C. A small fiber-optic temperature sensor is suggested and experimentally proven using refractive index liquid functionalized side-hole microstructured optical fibres (SHMOFs) [95]. The transmission spectrum of the suggested temperature sensor has been examined experimentally and theoretically. Multiple resonance dips in the transmission spectrum

Preprints (www.preprints.org) | NOT PEER-REVIEWED | Posted: 10 February 2023 doi:10.20944/preprints202302.0180.v1

are present due to resonance coupling between the fundamental core mode and refractive index liquid rod modes, which may be adjusted by modifying ambient temperature. According to the experimental data, the maximum temperature sensitivity is 13.1 nm/°C over a temperature range of 80-100 °C.

Zhang et al. [96] demonstrated surface plasmon resonance (SPR) based temperature sensor made of silver-coated multi-hole optical fiber. The structure of the proposed sensor is consisting of an input lead-in MMF, a silver-coated multi-hole optical fiber and an output lead-out MMF. The middle silver-coated multi-hole optical fiber (SMHOF) is filled with two types of thermo- sensitive liquid. In the previous reported sensors, the external temperature was monitored by measuring the wavelength shift of single SPR peak. However, the proposed work utilizes the concept of dual SPR dips which ultimately improves the sensitivity and expanded the detection range. Here, in a single optical fiber structure, two distinguish SPR dips at different wavelength which caused by adjusting refractive index of two types of thermo-sensitive liquid moves in opposite direction having some temperature difference are excited. The illustrative view of proposed SMHOF temperature sensor and the cross-section of thermos-sensitive liquid filled SMHOF are shown in Figure 8a,b respectively. A linear relationship between the environmental temperature and the interval of the two SPR dips is demonstrated. The reported SMHOF temperature sensors offer the high sensitivity of 7.72 nm/°C and -7.81 nm/°C in the range of 20-60 °C and -20-20 °C, respectively.

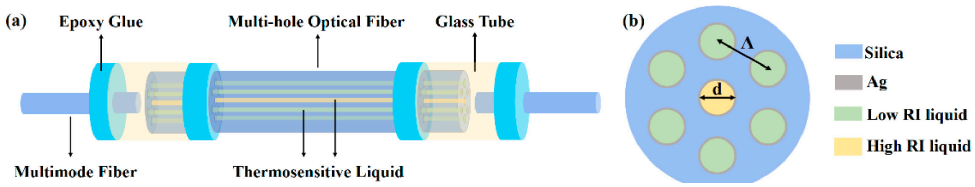

Figure 8. (a) Schematic diagram of the proposed SMHOF temperature sensor. (b) The cross-section of the SMHOF filled with thermo-sensitive liquids [96]. (Optics express).

3. Standard fiber

The last decade has shown the enormous interest in optical fibers used for sensing and long-distance operation applications. The optical fiber in sensors applied as a sensing element to monitor surrounding parameters like strain, pressure, vibration, temperature, etc. [97]. There are several ways of converting temperature signal into optical and then an electrical signal. The most popular used approach is to employ single-mode fiber (SMF), multimode fiber (MMF), tapered and etched fibers as temperature sensor. Other than this, the application of single-mode-multimode-single-mode fiber is being also utilized [98,99]. The integration of Mach-Zehnder interferometer (MZI), Fabry Perot interferometer (FPI) or Bragg grating on optic fiber is widely used for the sensing application [97 1]. The advantage associated with these systems is the capability to monitor temperature at every position and over long distances. However, each method has its own merits and demerits; few of these suffer from high cost, fabrication complexity and sophisticated equipment. In this section, the current status of research on SMF, MMF, tapered and etched fiber as temperature sensor is presented.

Wang et al. presented [100] a temperature sensor having single-mode-no-core-single-mode fiber structure with PDMS coating. In this work, PDMS due to its negative thermos-optic coefficient and large thermal expansion coefficient (TEC) is employed to increase the TEC of no-core optical fiber to finally enhance the temperature sensitivity of the proposed sensor. The study reports the result obtained using both theoretical analysis (MATLAB) and experiment. The schematic and physical diagram of the sensor is shown in in Figure 9.

Preprints (www.preprints.org) | NOT PEER-REVIEWED | Posted: 10 February 2023 doi:10.20944/preprints202302.0180.v1

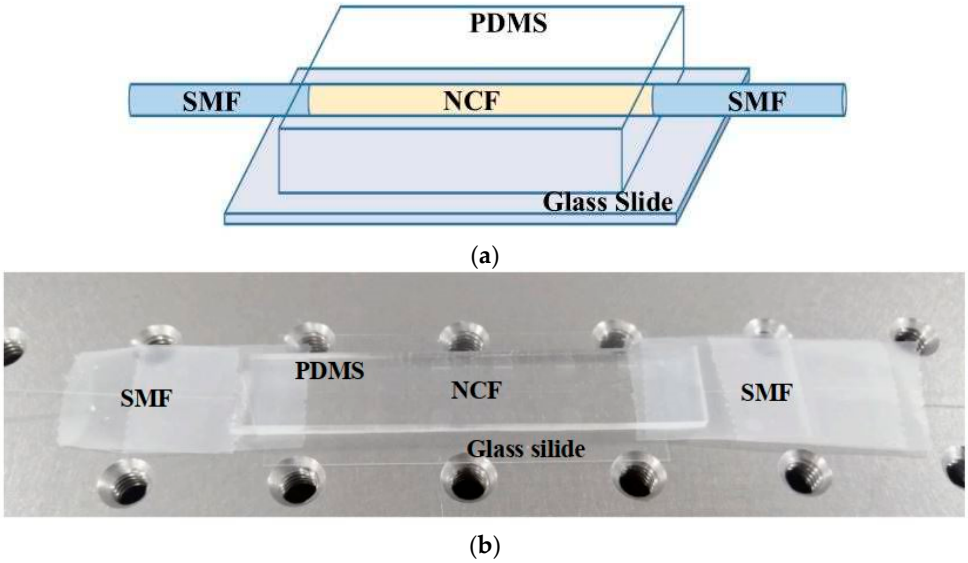

Figure 9. (a) Structural and (b) physical picture of sensor chip [100].

The theoretical finding is found to be in good agreement with the experimental results and the temperature sensitivity is – 260 pm/°C. In addition, the proposed sensor also offers strong resistance to external interference and mechanical damage, simple fabrication. In 2022, Xiaowei et al. [101] reported a sensor having arc-shaped misaligned structure MZI on a SMF.A layer of composite material (UV-curable polymer) is coated over the sensor to improve the temperature sensitivity. Along with temperature sensitivity, the strain sensitivity is also measured which found negligible. The proposed work shows the result from both theoretical analysis and experiment. Compared to previous reported sensors, the proposed temperature sensor shows an improved sensitivity which is -0.953nm/°C. Owing to simple manufacturing and small size, the proposed device may find its application in the domain of biology and chemistry. Similarly, Sun et al. [99] presented a sensor having single-mode fiber spliced with multimode fiber on which a Bragg grating structure has been written. The reported sensor with good reliability, repeatability and accuracy finds its application in the sensing of high temperature and micro-bending. Temperature and micro-bending's measurement range was defined as 0~900°C and 0~0.453m^{-1}. The temperature sensitivity and maximum bending sensitivity in the corresponding range was found to be 13.4 pm/°C and 23.03 dB/ m^{-1}. Similarly, the accuracy was measured as 0.002~0.005 dB.

In 2019, Huang et al. [102] proposed temperature and refractive index sensor based on multimode-single-mode-multimode fiber structure having graphene-metal hybrid coating over it. The sensitivity was improved by adding the graphene layer above or below of gold coating in fiber. It was found that the refractive index sensitivity of the Graphene-Gold-Au on Ag nanoparticle film is higher than the conventional Au on Ag nanoparticle film, Graphene-Au or Au-Graphene films. The sensitivity of graphene Au-Au@Ag NPs film (1591 nm/RIU) is higher than that of Au@Ag NPs (29 nm/RIU), graphene-Au (1224 nm/RIU), Au (1034 nm/RIU) and Au-graphene film (807 nm/RIU) modified MMF-SMF-MMF structure at the RI of 1.333. Similarly, polydimethylsiloxane (PDMS) has been added to the Graphene-Gold-Au on Ag nanoparticle film for sensing of temperature exhibiting the higher sensitivity of 1.02 nm/°C with good repeatability. The proposed sensor finds its application in protection, environmental, nano-medicine and cleans energy fields. Gao et al. [103] demonstrated an optical fiber based temperature sensor with PDMS/silica hybrid structure which is based on modal interference principle. The hybrid structure is placed between two single mode fibers that act as the sensing unit. Here, PDMS is integrated to enhance the sensitivity which is inserted into the hollow core fiber to ultimately develop PDMS/silica hybrid fiber structure. The illustrative sensor structure is shown in Figure 10. Here, the PDMS filled length, core diameter and air-gap length was taken as 20 mm, 30 um and 1 mm respectively.

Preprints (www.preprints.org) | NOT PEER-REVIEWED | Posted: 10 February 2023 doi:10.20944/preprints202302.0180.v1

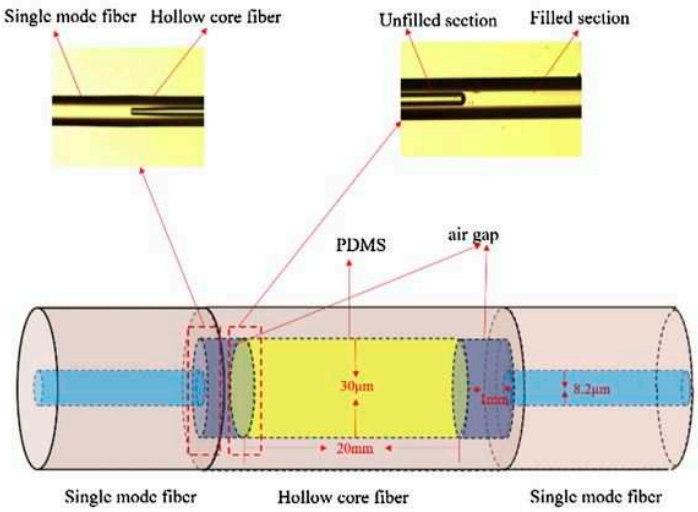

Figure 10. Temperature sensor with PDMS/silica hybrid fiber structure [103].

The hybrid fiber with different modes experiences the phase delay which is influenced by the external environmental conditions. Owing to the modal interference concept, the resonance wavelength shifted with respect to the variation in temperature. The experimental finding determined the sensor sensitivity to be −384 pm/°C for 25°C–80°C of range with the the hollow core fiber of core diameter of 30 um. The proposed temperature sensor can be used to sense the real time temperature in domains of Chemical, biological detection and medical. A similar work has been reported by Cai et al. [104] where they proposed an optical fiber based temperature sensor. The sensor follows the modal interference phenomenon of modes that occur in multimode fiber. The sensor includes the segment of single-mode fiber, hollow core fiber and no-core fiber with PDMS integrated over the cavity of hollow core fiber. The high thermo-optic coefficient and thermal-expansion coefficient of PDMS makes the effective refractive index to change larger with the change in temperature and hence makes a good temperature sensor. Both the experimental and simulation results have been presented where the experimentally obtained results found at par with the results obtained by simulation. A temperature sensitivity of 580.6 pm/°C in the range of 28°C to 50°C has been obtained.

In 2017, Peng et al. [105] reported a U-shaped bent single mode fiber based temperature sensor. The U-shaped fiber has a double coating of outer nickel protection coating and inner. A linear relation between temperature and bend loss at a fixed wavelength and bending radius has been presented. The inner coating worked as absorption coating and outer nickel coating worked as a protector of sensor. The proposed sensor offers temperature resolution and bends loss response of 0.5 °C and 0.023 dB/°C. Hence, the proposed sensor can also be used for monitoring temperature in harsh environment. Wildner et al. [106] shows the combination of two materials (glass particles and transparent oil/polymer) with different thermos-optic coefficient into the formation of temperature sensor. Here, the key performance parameters that varies the sensing of temperature such as particle size, filling degree and length are varied. The work demonstrated the freedom to select materials in according with the desired output of sensor. Small (large) differences in thermo-optic coefficient of two materials are selected for wide (small) measuring range. In a similar work, Noor et al. [107] proposed the use of SMF-MMF-SMF following the multimode interference phenomenon as temperature sensor. The bent MMF unit because of its small curvature radius projects a balloon shape. The MMF is coated with acrylate coating which offer higher temperature sensitivity due to its higher thermos-optic coefficient. The work reports both simulated and experimentally obtained results. In a temperature range of 27°C to 31°C, wavelength and intensity based interrogation and temperature sensitivity of -25.1 nW/°C and -2060 pm/°C respectively has been obtained. The work also points the importance of properly selecting the sensor dimension such as length of MMF, core

Preprints (www.preprints.org) | NOT PEER-REVIEWED | Posted: 10 February 2023 doi:10.20944/preprints202302.0180.v1

diameter and bending radius to further improve the temperature sensitivity. Hao et al. [108] using SMF core-offset structure developed a low-cost and simple temperature sensor. The schematic diagram of the sensor is shown in Figure 11. With the application of temperature over core-offset structure, the output laser wavelength due to variation in pass-band varies.

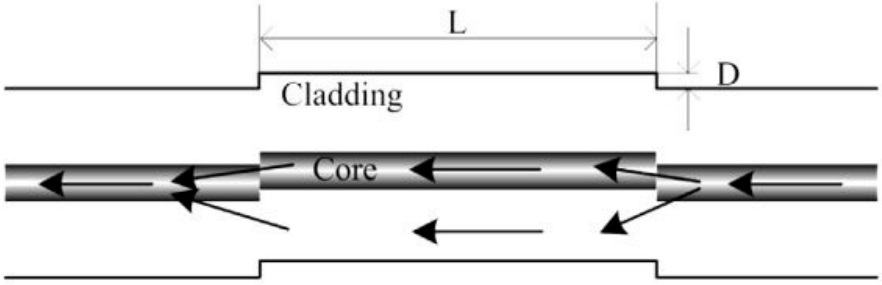

Figure 11. Schematic diagram of core-offset SMF based temperature sensor [108].

The experimental outcome shows the achievement of single-wavelength laser with the application of core-offset structure in the ring cavity. With the pump power of 100Mw, the output laser peak power and SMSR of -8.93 dB and 47 dB respectively has been found. For the temperature range of 30°C- 270°C, temperature sensitivity of 0.0449 nm/°C has been obtained. Compared to the previous reported sensors, the proposed sensor offered higher output power, higher SMSR, large measuring range and lower cost and therefore can find its application in laser sensing domain.

In 2013, Manoj et al. [109] presented a comparative study of temperature sensor developed using single-multi-single mode fiber using step and graded index multimode fibers. Here, GeO_2 with two different doping concentration has been employed in the core of multimode fiber. For the entire wavelength range of 0.7-1.6 μm, the temperature sensitivity of proposed sensor with graded index MMF was found larger (25-285 times) than the step-index MMF. In the same year, Yang et al. [110] liquid-sealed S-tapered fiber based highly sensitive temperature sensor. Here, the thermo-optic effect of liquid and thermal expansion of S-taper fiber makes the temperature sensor more sensitive. The length of the sensor can be varied from 10 mm to 1 mm. A detailed experimental analysis has been presented. The highly sensitive sensor with sensitivity of -1.403 nm/°C was demonstrated. For high temperature monitoring, Tan et al. [111] in the same year reported a partial-reflection-enabled compact Fabry-Perot interferometer (FPI) based sensor. The Fabry-Perot interferometer includes single mode fiber and a small core micro-structured fiber. It follows the basic principle of occuring partial Fresnel reflection at the interface of the two fibers and end surface of the micro-structured fiber. The compact and simple temperature sensor showed the response to high temperature such as 1000°C with the temperature sensitivity of 17.7 pm/°C at 1570 nm. The senor also finds its application in space-oriented high temperature monitoring applications. In 2012, Arun et al. [112] reported the design and fabrication of SMF-based temperature sensor developed using wet-etching method. A dependency of sensitivity on etched fiber diameter was found. The sensor showed an insensitive functioning of an un-etched fiber and 3.8 μW/°C (0.2 μW/°C) as the highest sensitivity for 11.2 μm (25 μm) etched diameter. The sensor outcome was found to be appropriate for analogue signal transmission over optical fiber through thermal modulation. In addition of these reviewed article some other article utilzied these standard fibers to achieve supirior sensing performance as shown in Table 1.

Table 1. Summary of other standard optical fiber based temperature sensors.

Fiber structure	Material	Temp. range	Sensitivity	Refs.
SMF-MMF	N/A	0-900°C	13.4pm/°C	[99]
SMF-NCF-SMF	N/A	N/A	– 260 pm/°C	[100]
arc-shaped misaligned MZI on SMF	N/A	N/A	-0.953nm/°C	[101]

Preprints (www.preprints.org) | NOT PEER-REVIEWED | Posted: 10 February 2023 doi:10.20944/preprints202302.0180.v1

MMF-SMF-MMF	PDMS on graphene Au-Au@Ag NPs	N/A	1.02 nm/°C	[102]
SMF-HCF-SMF	PDMS	25°C–80°C	−384 pm/°C	[103]
SMF-NCF-SMF	PDMS	28°C–50°C	580.6 pm/°C	[104]
SMF-MMF-SMF	N/A	27°C–31°C	-2060 pm/°C	[107]
core-offset SMF	N/A	30°C–270°C	0.0449 nm/°C	[108]
S-tapered fiber	N/A	--	-1.403 nm/°C	[110]
FPI in SMF	N/A	1000°C	17.7 pm/°C	[111]
SMF-SCPSF-SMF	N/A	200°C - 1000°C	106.64 pm/°C	[113]
multimode POF	N/A	25°C - 110°C	1.04×10^{-3}°C^{-1}	[114]
FBGs embedded in PLA	N/A	20°C - 70°C	139 pm/°C	[115]

4. Grating based fiber

Nowadays, the fiber Bragg grating（FBG）are considered as one of the most popular optical components which are widely exploited in optical networking, physical and chemical sensing due to their ease of fabrication, small size, multiplexing feature, and low cost. An FBG comprises a periodic variation of the refractive index (RI) within the core of a single-mode fiber, which satisfies the phase matching condition between the fundamental mode and other modes, either the core mode or the cladding modes or radiation (or leaky) modes [116]. In 1978, Hill *et al.* fabricated and reported first FBG in germanium-doped core [117]. The grating was made by using laser lithography technique to incorporate the permanent periodic variation of the refractive index in fiber core.

The sensing principle of FBG based fibers can be defined as the grating period, grating length, and the effective refractive index of such fibers that are affected by the variation in the surrounding media [118]. The change in the outer environment leads to the change in its resonance condition; consequently, the variation in resonance wavelength takes place. Based on the property of these gratings, it can be classified into three categories: (1) fiber Bragg grating (FBG), (2) long-period fiber grating (LPFG), and (3) tilted FBG (TFBG). The grating based optical fibers gains huge attention in physical and chemical sensing due to their unique features of immunity to electromagnetic interferences, compact size, highly sensitive, multiplexing capability and *in-situ* monitoring. Owing to their design of label-free monitoring of surrounding environment the grating-based sensors, such as FBG, LPG, etched FBG, and TFBG, have attracted extensive attention in order to develop physical and chemical sensors. In the grating based fibers, the Bragg wavelength is calculated by the refractive index modulation period (L) and the effective refractive index of the fiber (n_{eff}), and shown by following relation:

$$\boldsymbol{\lambda_{Bragg} = 2n_{eff}L} \qquad (1)$$

A change in the refractive index of the fiber is observed, under the variation of the temperature, leading to a linear drift in the value of the Bragg wavelength. Temperature monitoring using grating fibers can be easily achieved by demodulating the Bragg wavelength variation. Compared to other optical fiber sensors, the grating based temperature sensors showed several advantages including good linearity, high stability, multiplexing capability, mass production, etc., which have been used widely in commercialization.

In 2014, Zaynetdinov *et al.* developed a FBG based temperature sensor operated ranging from 2–400 K. along with a temperature resolution better than 10 mK for temperatures below than 12 K [119]. The sensing head was fabricated from polyimide coated optical fiber. The response was achieved by mounting the section of the fiber on a polytetrafluoroethylene tape, which has a non-negligible coefficient of thermal expansion down to <4 K. The sensors exhibited an excellent stability over multiple trials along with the superior repeatability of temperature cycles. In 2016, Hsiao *et al.* reported a chromium nitride (CrN) coated FBG sensor for extreme temperature environments [120].

Preprints (www.preprints.org) | NOT PEER-REVIEWED | Posted: 10 February 2023 doi:10.20944/preprints202302.0180.v1

The sensing configuration was fabricated by depositing CrN using physical vapor deposition (PVD) technique. During the sputtering process the pressure of the deposition system was fixed at 6×10^{-3} Torr with 70 W power applied to the Cr target. The film was deposited for 15 min to achieve an approximate thickness of 2 μm over the FBG. The sensor was based on wavelength interrogation technique anlayzed by utilizing an optical spectrum analyzer (OSA). The reflection spectra of the fabricated sensor were monitored and compared with bare FBG for temperatures varying from 100 °C to 650 °C. The results exhibited that the CrN-coated FBG sensor gives a 14.0 pm/°C greater temperature sensitivity compared to the bare FBG fiber without CrN.

In 2018, Dong *et al.* reported the utilization of graphene oxide (GO) as sensing layer integrated over FBG for simultaneous pressure and temperature monitoring [121]. The sensing configuration was based on Fabry–Perot interferometer (FPI). The light reflectors of the fabricated FPI sensor comprise with a thin graphene film coated over end facet of FBG, as shown in Figure 12. The sensor exhibited good sensitivities of 501.4 nm/kPa and 306.2 nm/°C, for pressure and temperature, respectively. The introduction of FBG along with GO can successfully prevent the cross-impact of the FPI sensor. Following the improvement of sensing performance, in same year of 2018, Jasmi *et al.* also reported an FBG based temperature sensor by utilizing polyurethane-GO nanocomposite as sensing layer [122]. The physical, chemical, and conductivity of PU-GO were observed to be improved after introducing GO in the pristine PU. The thermogravimetric analysis exhibited that the thermal stability of PU improved to 217 °C because of the strong intermolecular interaction with graphene flakes leading to an enhanced in sensing performance. The sensing material was coated over FBG using dip-coating to get uniform thickness, while the sensing performance of the device was evaluated for a wide range of temperature varying from 25 to 60 °C. The sensor exhibited a good linearity along with an improved sensitivity of 6 pm/°C.

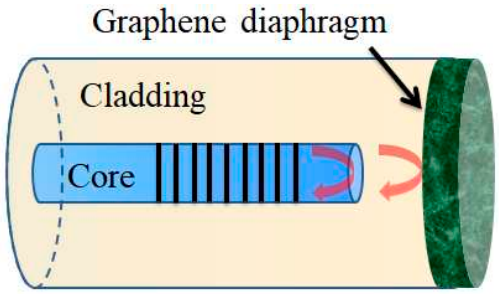

Figure 12. FBG sensor integrated with graphene for simultaneous detection of temperature and pressure.

In 2019, Cheng et al introduced strontium titanate ($SrTiO_3$) thin film coated over FBG using pulsed laser deposition for temperature sensing [123]. $SrTiO_3$ is an ferroelectric thin films with an typical perovskite like structures with remarkable optical, dielectric, and photoelectric properties. For deposition the FBG was immersed in the acetone solution for 5 min to remove the buffer coating, which was later coated with 271.5 nm thick $SrTiO_3$ film on the cladding. In order to study the thermal sensing performance of the FBG, a concatenated optical path, two optical paths based on a Michelson interferometer (MI) and one based on Sagnac interferometer (SI), were fabricated using $SrTiO_3$ coated FBG and another bare FBG. The sensing performance of the device was investigated for a wide range of temperature varying from 40 °C to 150 °C. The sensitivity for each sensing configuration was observed to be 9.0 pm/°C, 10.5 pm/°C and 11.4 pm/°C, for two MI and one SI, respectively. Later in 2020, Gao *et al.* reported an dual-parameter fiber sensor consist of a few-mode fiber and FBG for simultaneous detection of strain and temperature variation [124]. The sensing configuration was fabricated using 6.5 cm length of few mode fiber offset spliced with single-mode fiber (SMF), as shown in Figure 13. The temperature and strain were measured simultaneously due to the different sensitivities of the obtained spectrum dips. The fabricated sensor exhibited a good temperature sensitivities of -34.3 pm/°C and 10.7 pm/°C, while the strain sensitivities of -2 pm/$\mu\varepsilon$ and 0.67 pm/$\mu\varepsilon$,

Preprints (www.preprints.org) | NOT PEER-REVIEWED | Posted: 10 February 2023 doi:10.20944/preprints202302.0180.v1

respectively. The fabricated device showed good potential in fields of the dual-parameter measurement due to its simple configuration, cost effectiveness and compact structure.

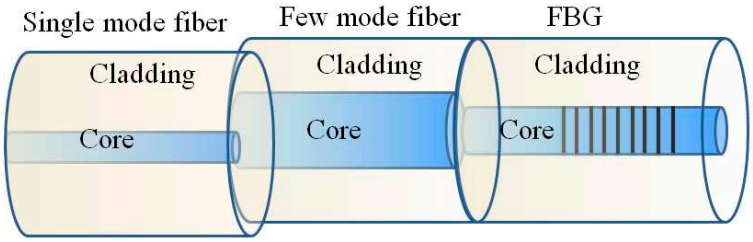

Figure 13. Sensing configuration for strain and temperature monitoring.

Later in 2021, Chen *et al.* reported an optical fiber sensor based on a fiber surface waveguide and Bragg grating for a simultaneous monitoring of refractive index and temperature variations [125]. The device consists of two fiber Bragg gratings fabricated by a femtosecond laser, one of which is situated in the fiber core for temperature sensing; the other is located in the fiber surface waveguide for both temperature and RI measurements. The fabricated device exhibited a good RI and temperature sensitivities of 10.3 nm/RIU and 9.94 pm/°C, respectively. Later in 2022, Esposito *et al.* reported a miniaturized metallic package for FBG sensors to improve the temperature sensitivity and eliminate the cross-sensitivities to mechanical effects of impulsive forces or strain [126]. The packaging of device required the encapsulation of FBG into a steel tube, which was later placed inside another larger steel tube, where the fiber was kept loose to prevent any mechanical effect transferring to the grating. The fabricated device exhibited a linear temperature response in the range varying from 5 °C to 50 °C along with a high sensitivity of 28.9 pm/ °C, which was nearly three times higher than the standard FBG. In addition to sensing performance the device also shows a rapid response time of 5 s when tested under temperature of 20 °C. In addition of these reported FBG based sensors, some other sensor also listed in Table 2 which shows an excellent performance and competitive response.

Table 2. Summary of FBG based temperature sensors.

Fiber structure	Material	Temp. range	Sensitivity	Refs.
FBG	N/A	5-50 °C	28.9 pm/ °C	[126]
FBG	N/A	27–427 °C	14.42 pm/°C	[127]
FBG	N/A	-5 – 35 °C	35 mV/°C	[128]
Sapphire-FBG	N/A	0-1800 °C	41.2 pm/°C	[129]
Sapphire-FBG	N/A	0-1200 °C	30.19 pm/°C	[130]
FBG	N/A	0-1000 °C	18.2 pm/°C	[131]
FBG	N/A	40-260 °C	13 pm/°C	[132]
FBG	Titanium nitride	25 to −195 °C	10.713 pm/ °C	[133]
Tapered FBG	Gold	0-50 °C	9.893 pm/°C	[134]
Hollow core Bragg fiber	N/A	600 °C	25.925 pm/°C	[135]
FBG	poly (methyl methacrylate)	15-35 °C	−0.080 nm/°C	[136]
FBG	polydimethylsiloxane	20, 30, 40 and 50 °C	4.88, 5.15, 4.53 and 4.38 nm/°C	[137]
FBG	Polymer	80 °C	9.33 nm/°C	[138]

5. Future prospects and challenges:

With the advancement of micro- and nano-technology and the development of fibres with unique optical characteristics, there is little question that designs and fabrications of innovative micro-structured fibre optic sensors will continue to be a thriving research topic. Opportunities and challenges are coexisting simultaneously in the work to be done on micro-structured fibre optic sensors in the future. It includes ability to measure multiple parameters simultaneously and with selectivity: Although several micro-structured fibre optic sensors with dual-parameter measuring capabilities have been proposed to date, efforts should be made to reduce measurement error and expand dual-parameter measurement to three-parameter or even more parameter characterizations because crosstalk effect is typically brought on by more than two parameters in many applications. Even greater sensitivity also requires for the MOF sensors with exceptionally high accuracies for more exact measurements. Sensing in severe conditions is require including those with high pressure, strong radiation, and extremely low or high temperatures. An intelligent MOF sensor should have functionalities that can be changed and adjusted in response to various target samples and circumstances. A more adaptable and potent sensor architecture would be desirable. The robustness of the microscopic structures is the key to the sensing performance and longevity of the device, therefore a better packaging without sacrificing sensitivity will be the future goal. Also, there is need of simplified and easy fabrication process for the MOF sensor. One main aspects of the MOF based sensor is to control the attenuation loss which is more important for the practical application.

Real time monitoring of temparatures in patients in inpatient floor and ICU with small devices that can monitor the fluctuations in real time same as telemetry can be extremely useful in patients with pneumonia and or sepsis and any other infections especially those who are intubated and unable to speak in critical care units. It will make more efficient detection of hospital acquired infections and will be helpful for quicker reaction to tackle possible infection in patients. In a normal clinical setting, patient has to inform the nurse that they have a fever or the nurse has to keep checking the temperature of the patient at regular intervals. With a real-time temparature monitoring device it would be easier and faster to catch a new infection and nip it in the bud before it goes to form a major infection or abscess and maybe useful in ultimately reducing a lot of incidences of sepsis.

Temperature monitoring is many times overlooked in critical care when compared to other factors such as pulse oximetry and telemetry but it is a important factor, a biological alarm that signals infection or some other abnormality in the patient. So this technology can be extremely useful in not only detecting cases of Covid or flu during pandemics for screening large number of people easily but it can also provide a means to monitor critically ill patients and give the doctors a head start in treating the infection before it become worse. This can revolutionise not just Screening but also patient monitoring.

6. Conclusion

In this review article, the role of various types of optical fibers and their sensing approach along with the sensor design, sensing material, working principle, and sensing performance including selectivity, sensitivity, and linearity are discussed and presented in detail. This paper provides a comprehensive reviews over the development of optical fiber based temperature sensors in past decades. Each sensing configuration comprises different structures and sensing material to achieve high sensitivity which is listed and discussed for each sensor. The new idea and approaches to improve the sensing performance of such devices are also suggested in future prospects section. Today, the increasing growth in the fields of optics, electronics, materials science, and data analysis has opened up a new path for the study which can be expanded to include these principles for high precision and accuracy.

Author Contributions: Conceptualization, AKP, SK; methodology, RKG, AKP, SK; validation, AKP, SK; formal analysis, RKG, AKP, SK, SDG; writing—original draft preparation, RKG,SK,AKP, SDG, MCM; writing—review and editing, RKG, AKP, SK; supervision, RKG, SK; project administration, AKP. All authors have read and agreed to the published version of the manuscript.

Funding: This research received no external funding.

Institutional Review Board Statement: Not applicable.

Informed Consent Statement: Not applicable.

Data Availability Statement: Not applicable.

Acknowledgments: Not applicable.

Conflicts of Interest: The authors declare no conflict of interest.

References

1. Ma, S.; Xu, Y.; Pang, Y.; Zhao, X.; Li, Y.; Qin, Z.; Liu, Z.; Lu, P.; Bao, X. Optical Fiber Sensors for High-Temperature Monitoring: A Review. *Sensors* **2022**, *22*, 5722, doi:10.3390/s22155722.
2. Childs, P. R. N.; Greenwood, J. R.; Long, C. A. Review of temperature measurement. *Rev. Sci. Instrum.* **2000**, *71*, 2959–2978, doi:10.1063/1.1305516.
3. Yang, S.; Homa, D.; Heyl, H.; Theis, L.; Beach, J.; Dudding, B.; Acord, G.; Taylor, D.; Pickrell, G.; Wang, A. Application of Sapphire-Fiber-Bragg-Grating-Based Multi-Point Temperature Sensor in Boilers at a Commercial Power Plant. *Sensors* **2019**, *19*, 3211, doi:10.3390/s19143211.
4. Willsch, M.; Bosselmann, T.; Flohr, P.; Kull, R.; Ecke, W.; Latka, I.; Fischer, D.; Thiel, T. Design of fiber optical high temperature sensors for gas turbine monitoring. In; Jones, J. D. C., Ed.; 2009; p. 75037R.
5. Atkins, R. A.; Gardner, J. H.; Gibler, W. N.; Lee, C. E.; Oakland, M. D.; Spears, M. O.; Swenson, V. P.; Taylor, H. F.; McCoy, J. J.; Beshouri, G. Fiber-optic pressure sensors for internal combustion engines. *Appl. Opt.* **1994**, *33*, 1315, doi:10.1364/AO.33.001315.
6. Watson, J.; Castro, G. A review of high-temperature electronics technology and applications. *J. Mater. Sci. Mater. Electron.* **2015**, *26*, 9226–9235, doi:10.1007/s10854-015-3459-4.
7. Gao, S.; Wang, L.; Feng, C. Multi-spectral pyrometer for gas turbine blade temperature measurement. Proc. SPIE 9202, Photonics Applications for Aviation, Aerospace, Commercial and Harsh Environments V, Eds.; 2014; p. 920217. https://doi.org/10.1117/12.2059424.
8. Zhang, L.; Zhu, Y.; Jiang, M.; Wu, Y.; Deng, K.; Ni, Q. Body Temperature Monitoring for Regular COVID-19 Prevention Based on Human Daily Activity Recognition. *Sensors* **2021**, *21*, 7540, doi:10.3390/s21227540.
9. Costanzo, S.; Flores, A. A Non-Contact Integrated Body-Ambient Temperature Sensors Platform to Contrast COVID-19. *Electronics* **2020**, *9*, 1658, doi:10.3390/electronics9101658.
10. Bielska, S.; Sibinski, M.; Lukasik, A. Polymer temperature sensor for textronic applications. *Mater. Sci. Eng. B* **2009**, *165*, 50–52, doi:10.1016/j.mseb.2009.07.014.
11. Wawrzynczyk, D.; Bednarkiewicz, A.; Nyk, M.; Strek, W.; Samoc, M. Neodymium(iii) doped fluoride nanoparticles as non-contact optical temperature sensors. *Nanoscale* **2012**, *4*, 6959, doi:10.1039/c2nr32203j.
12. Kus, A.; Isik, Y.; Cakir, M.; Coşkun, S.; Özdemir, K. Thermocouple and Infrared Sensor-Based Measurement of Temperature Distribution in Metal Cutting. *Sensors* **2015**, *15*, 1274–1291, doi:10.3390/s150101274.
13. Jun, S.; Kochan, O. Investigations of Thermocouple Drift Irregularity Impact on Error of their Inhomogeneity Correction. *Meas. Sci. Rev.* **2014**, *14*, 29–34, doi:10.2478/msr-2014-0005.
14. Nie, B.; He, X.; Zhang, C.; Li, X.; Li, H. Temperature measurement of gas explosion flame based on the radiation thermometry. *Int. J. Therm. Sci.* **2014**, *78*, 132–144, doi:10.1016/j.ijthermalsci.2013.12.010.
15. Pathak, A. K.; Viphavakit, C. A review on all-optical fiber-based VOC sensors: Heading towards the development of promising technology. *Sensors Actuators A Phys.* **2022**, *338*, 113455, doi:10.1016/j.sna.2022.113455.
16. Mollah, M. A.; Islam, S. M. R.; Yousufali, M.; Abdulrazak, L. F.; Hossain, M. B.; Amiri, I. S. Plasmonic temperature sensor using D-shaped photonic crystal fiber. *Results Phys.* **2020**, *16*, 102966, doi:10.1016/j.rinp.2020.102966.
17. Wang, Z.; Chen, D.; Yang, X.; Liang, S.; Sun, X. Temperature sensor of single-mode-no-core-single-mode fiber structure coated with PDMS. *Opt. Fiber Technol.* **2022**, *68*, 102793, doi:10.1016/j.yofte.2021.102793.
18. Liao, C. R.; Wang, D. N. Review of femtosecond laser fabricated fiber Bragg gratings for high temperature sensing. *Photonic Sensors* **2013**, *3*, 97–101, doi:10.1007/s13320-012-0060-9.
19. W. Wildner and D. Drummer, "A Fiber Optic Temperature Sensor Based on the Combination of Two Materials With Different Thermo-Optic Coefficients," in IEEE Sensors Journal, vol. 16, no. 3, pp. 688-692, Feb.1, 2016.
20. R. Kashyap, Fiber Bragg Gratings (Elsevier, Amsterdam, 1999).
21. Mizuno Y., Zou, W., He, Z., and Hotate, K., Proposal of Brillouin optical correlation –domain reflectometry (BOCDR). *Opt. Exp*. **2008,** 16, 12148, https://doi.org/10.1364/OE.16.012148.
22. A. H. Hartog, An Introduction to Distributed Optical Fibre Sensors (CRC Press, Boca Raton, FL, 2017).
23. G. Rajan (ed.) Optical Fiber Sensors: Advanced Techniques and Applications (CRC Press, Boca Raton, FL, 20154).

24. H. Alemohammad, Opto-Mechanical Fiber Optic Sensors: Research, Technology, and Applications in Mechanical Sensing (Elsevier, Amsterdam, 2018).
25. P. Russell, "Photonic crystal fibers," Science 299, 358–362 (2003).
26. 7. J. C. Knight, "Photonic crystal fibres," Nature 424, 847–851 (2003).
27. T. Larsen, A. Bjarklev, D. Hermann, and J. Broeng, "Optical devices based on liquid crystal photonic bandgap fibres," Opt. Exp., vol. 11, no. 20, pp. 2589–2596, Oct. 2003.
28. F. Du, Y. Lu, and S. Wu, "Electrically tunable liquid-crystal photonic crystal fiber," Appl. Phys. Lett., vol. 85, pp. 2181–2183, Sep. 2004.
29. M. Haakestad, "Electrically tunable photonic bandgap guidance in a liquid-crystal-filled photonic crystal fiber," IEEE Photon. Technol. Lett., vol. 17, no. 4, pp. 819–821, Apr. 2005.
30. T. Alkeskjold, J. Lægsgaard, A. Bjarklev, D. Hermann, A. Anawati, J. Broeng, J. Li, and S. T. Wu, "All-optical modulation in dye-doped nematic liquid crystal photonic bandgap fibers," Opt. Exp., vol. 12, no. 24, pp. 5857–5871, Nov. 2004.
31. P. Steinvurzel, B. Eggleton, C. D. Sterke, and M. J. Steel, "Continuously tunable bandpass filtering using high-index inclusion microstructured optical fibre," Electron. Lett., vol. 41, no. 8, pp. 463–464, Apr. 2005.
32. T. T. Alkeskjold and A. Bjarklev, "Electrically controlled broadband liquid crystal photonic bandgap fiber polarimeter," Opt. Lett., vol. 32, no. 12, pp. 1707–1709, Jun. 2007.
33. W. Qian, C. Zhao, Y. Wang, C. Chan, S. Liu, and W. Jin, "Partially liquid-filled hollow-core photonic crystal fiber polarizer," Opt. Lett., vol. 36, no. 16, pp. 3296–3298, Aug. 2011.
34. R. Jha, J. Villatoro, G. Badenes, and V. Pruneri, "Refractometry based on a photonic crystal fiber interferometer," Opt. Lett., vol. 34, no. 5, pp. 617–619, Mar. 2009.
35. B. Li, Z. Sheng, M. Wu, X. Liu, G. Zhou, J. Liu, Z. Hou, and C. Xia, "Sensitive real-time monitoring of refractive indices and components using a microstructure optical fiber microfluidic sensor," Optics letters, Vol. 43, no. 20, pp. 5070-5073, 2018.
36. A. Canales, X. Jia, U. P. Froriep, R. A. Koppes, C. M. Tringides, J. Selvidge, C. Lu, C. Hou, L. Wei, T. Fink and P. Anikeeva, "Multifunctional fibers for simultaneous optical, electrical and chemical interrogation of neural circuits in vivo," Nature biotechnology, vol. 33, no. 3, pp. 277, 2015.
37. Xuefeng Li, Shuo Lin, Jinxing Liang, Yupeng Zhang, Hiroshi Oigawa, and Toshitsugu Ueda, "Fiber-Optic Temperature Sensor Based on Difference of Thermal Expansion Coefficient Between Fused Silica and Metallic Materials," IEEE Photonics Journal, vol. 4, no. 1, pp. 155-162, 2012
38. Erick Reyes-Vera, Cristiano M. B. Cordeiro, and Pedro Torres, "Highly sensitive temperature sensor using a Sagnac loop interferometer based on a side-hole photonic crystal fiber filled with metal," Applied Optics, Vol. 56, Issue 2, pp. 156-162 ,2017.
39. H. Yang, S. Wang, X. Liao, and J. Wang, "Temperature sensing in seawater based on microfiber knot resonator," Sensors (Basel), vol. 14, no. 10, pp. 18515-18525, 2014.
40. Y. Lu, M. T. Wang, C. J. Hao, Z. Q. Zhao, and J. Q. Yao, "Temperature Sensing Using Photonic Crystal Fiber Filled With Silver Nanowires and Liquid," IEEE Photonics J, vol. 6, no. 3, pp. 1-7, 2014.
41. Erick Reyes-Vera, Nelson D. Gómez-Cardona, Giancarlo Chesini, Cristiano M. B. Cordeiro, and Pedro Torres, "Temperature sensibility of the birefringence properties in side-hole photonic crystal fiber filled with Indium," Appl. Phys. Lett, vol. 105, Issue 20, p1,2014
42. Wenwen Qian, Chun-Liu Zhao, Shaoling He, Xinyong Dong, Shuqin Zhang, Zaixuan Zhang, Shangzhong Jin, Jiangtao Guo, and Huifeng Wei, "High-sensitivity temperature sensor based on an alcohol-filled photonic crystal fiber loop mirror," Optics Letters, vol. 36, no. 9, pp. 1548-1550, 2011
43. Giancarlo Chesini, Jonas H. Osório, Valdir A. Serrão, Marcos A.R. Franco, and Cristiano M. B. Cordeiro, "Metal-Filled Embedded-Core Capillary Fibers as Highly Sensitive Temperature Sensors," IEEE Sensors Letters, vol. 2, no. 2, 2018
44. J. Xie, B. Xu, Y. Li, J. Kang, C. Shen, J. Wang, Y. Jin, H. Liu, K. Ni, X. Dong, C. Zhao, and S. Jin, "High-sensitivity temperature sensor based on a droplet-like fiber circle," Appl. Opt, vol. 53, no. 18, pp. 4085-4088, 2014.
45. W. Qian, C. L. Zhao, S. He, X. Dong, S. Zhang, Z. Zhang, S. Jin, J. Guo, and H. Wei, "High-sensitivity temperature sensor based on an alcohol filled photonic crystal fiber loop mirror," Opt. Lett, vol. 36, no. 9, pp. 1548-1550, 2011.
46. Dora Juan Juan Hu, Jun Long Lim, Ying Cui, Karolina Milenko, Yixin Wang, Perry Ping Shum, and Tomasz Wolinski, "Fabrication and Characterization of a Highly Temperature Sensitive Device Based on Nematic Liquid Crystal-Filled Photonic Crystal Fiber," IEEE Photonics Journal, vol. 4, no. 5, pp. 1248-1255, 2012.
47. Tong Chen, Qingqing Wang, Rongzhang Chen, Botao Zhang, Charles Jewart, Kevin P. Chen, Mokhtar Maklad, and Phillip R. Swinehart, "Distributed high-temperature pressure sensing using air-hole microstructural fibers," Opt. Lett. 37, 1064-1066 (2012).
48. Xiaolei Li, Qizhen Sun, Duan Liu, Ruibing Liang, Jiejun Zhang, Jianghai Wo, Perry Ping Shum, and Deming Liu, "Simultaneous wavelength and frequency encoded microstructure based quasi-distributed temperature sensor" OPTICS EXPRESS, 20(11), 12076-12084, 2012.

49. Xiaoling Tan, Youfu Geng, Xuejin Li, Rong Gao, and Zhen Yin, "High temperature microstructured fiber sensor based on a partial-reflection-enabled intrinsic Fabry–Perot interferometer", Applied Optics, 52 (34), 8195-8198, 2013.
50. C. G. Poulton, M. A. Schmidt, G. J. Pearce, G. Kakarantzas, and P. S. Russell, "Numerical study of guided modes in arrays of metallic nanowires," Opt. Lett. 32, 1647–1649 (2007).
51. J. Hou, D. Bird, A. George, S. Maier, B. Kuhlmey, and J. C. Knight, "Metallic mode confinement in microstructured fibres," Opt. Express 16, 5983–5990 (2008).
52. M. A. Schmidt, L. N. P. Sempere, H. K. Tyagi, C. G. Poulton, and P. S. J. Russell, "Waveguiding and plasmon resonances in two-dimensional photonic lattices of gold and silver nanowires," Phys. Rev. B 77, 033417 (2008).
53. P. J. A. Sazio, A. Amezcua-Correa, C. E. Finlayson, J. R. Hayes, T. J. Scheidemantel, N. F. Baril, B. R. Jackson, D. J. Won, F. Zhang, and E. R. Margine, "Microstructured optical fibers as high-pressure microfluidic reactors," Science 311, 1583–1586 (2006).
54. J. A. Harrington, "A review of IR transmitting, hollow waveguides," Fiber Integr. Opt. 19, 211–227 (2000).
55. F.C. Favero et al., "Microstructure fiber interferrometer as sensitive temperature measurement," Photonic Sensor, 3, 208-213 (2013).
56. Luan, N.; Wang, R.; Lv, W.; Lu, Y.; Yao, J. Surface Plasmon Resonance Temperature Sensor Based on Photonic Crystal Fibers Randomly Filled with Silver Nanowires. *Sensors* **2014**, *14*, 16035-16045.
57. Nan-Nan Luan, Ran Wang, Ying Lu, and Jianquan Yao, "Simulation of Surface Plasmon resonance temperature sensor based on liquid mixture-filling microstructured optical fiber", Optical Engineering, 53(6), 067103, 2014.
58. Youfu, G.; Xuejin, L.; Xiaoling, T.; Yuanlong, D.; Xueming, H. Compact and Ultrasensitive Temperature Sensor With a Fully Liquid-Filled Photonic Crystal Fiber Mach-Zehnder Interferometer. *IEEE Sens. J.* 2014, *14*, 167–170.
59. Du, Y.; Qiao, X.; Ronjg, Q.; Yang, H.; Feng, D.; Wang, R.; Hu, M.; Feng, Z. A miniature Fabry-Pérot Interferometer for High Temperature Measurement Using a Double-Core Photonic Crystal Fiber. *IEEE Sens. J.* 2014, *14*, 1069–1072.
60. Ding, W.H.; Jiang, Y. Miniature Photonic Crystal Fiber Sensor for High-Temperature Measurement. *IEEE Sens. J.* 2014, *14*, 786–789.
61. Lopez-Aldaba, A.; Pinto, A.M.R.; Lopez-Amo, M.; Frazão, O.; Santos, J.L.; Baptista, J.M.; Baierl, H.; Auguste, J.-L.; Jamier, R.; Roy, P. Experimental and Numerical Characterization of a Hybrid Fabry-Pérot Cavity for Temperature Sensing. *Sensors* 2015, *15*, 8042-8053. https://doi.org/10.3390/s150408042
62. Scarcia, W.; Palma, G.; Falconi, M.C.; De Leonardis, F.; Passaro, V.M.N.; Prudenzano, F. Electromagnetic Modelling of Fiber Sensors for Low-Cost and High Sensitivity Temperature Monitoring. *Sensors* **2015**, *15*, 29855-29870. https://doi.org/10.3390/s151229770
63. R. A. Pérez-Herrera, R.M. André, S.F. Silva, M. Becker, K. Schuster, J. Kobelke, M. Lopez-Amo, J.L. Santos, O. Frazão, Simultaneous measurement of strain and temperature based on clover microstructured fiber loop mirror, Measurement, 65, 2015, Pages 50-53, https://doi.org/10.1016/j.measurement.2014.12.052.
64. S. Revathi, Srinivasa Rao Inabathini, Jatin Pal, "Pressure and temperature sensor based on a dual core photonic quasi-crystal fiber," Optik, 126(22), 3395-3399, 2015, https://doi.org/10.1016/j.ijleo.2015.07.141.
65. Lopez-Aldaba, A.; Pinto, A.M.R.; Lopez-Amo, M.; Frazão, O.; Santos, J.L.; Baptista, J.M.; Baierl, H.; Auguste, J.-L.; Jamier, R.; Roy, P. Experimental and Numerical Characterization of a Hybrid Fabry-Pérot Cavity for Temperature Sensing. *Sensors* **2015**, *15*, 8042-8053. https://doi.org/10.3390/s150408042.
66. Liu, Q., Li, S., Chen, H., Li, J., Fan, Z.: High-sensitivity plasmonic temperature sensor based on photonic crystal fiber coated with nanoscale gold film. Appl. Phys. Express **8**(4), 046701 (2015a)
67. Liu, Q., Li, S., Chen, H., Fan, Z., Li, J.: Photonic crystal fiber temperature sensor based on coupling between liquid-core mode and defect mode. IEEE Photonics J. **7**(2), 4500509 (2015b).
68. Wang, Q., Du, C., Zhang, J., Lv, R., Zhao, Y.: Sensitivity-enhanced temperature sensor based on PDMS-coated long period fiber grating. Opt. Commun. **377**, 89–93 (2016).
69. Liu, C.; Wang, F.; Lv, J.; Sun, T.; Liu, Q.; Fu, C.; Mu, H.; Chu, P.K. A highly temperature-sensitive photonic crystal fiber based on surface plasmon resonance. *J. Sci. Opt. Commun.* 2016, *359*, 378–382.
70. Du, C.; Wang, Q.; Zhao, Y.; Li, J. Highly sensitive temperature sensor based on an isopropanol-filled photonic crystal fiber long period grating. *J. Sci. Opt. Fiber Technol.* 2016, *34*, 12–15.
71. Stephen C. Warren-Smith, Linh Viet Nguyen, Catherine Lang, Heike EbendorffHeidepriem, and Tanya M. Monro, "Temperature sensing up to 1300°C using suspended-core microstructured optical fibers" Optics Express, 24(4), 3714-3719, 2016, DOI:10.1364/OE.24.003714.
72. Linh Viet Nguyen, Stephen C. Warren-Smith, Heike Ebendorff-Heidepriem, and Tanya M. Monro, "Interferometric high temperature sensor using suspended-core optical fiber", Optics Express, 24(8), 8967-8977, 2016. DOI:10.1364/OE.24.008967.

73. Erick Reyes-Vera, Cristiano M. B. Cordeiro, and Pedro Torres, "Highly sensitive temperature sensor using a Sagnac loop interferometer based on a side-hole photonic crystal fiber filled with metal," Appl. Opt. 56, 156-162 (2017)
74. Li, S., Xia, L., Chen, Z. *et al.* Colloidal crystal cladding fiber based on side-polished fiber and its temperature sensing. *Opt Quant Electron* 49, 66 (2017). https://doi.org/10.1007/s11082-017-0905-y.
75. Xu, Y.; Lu, P.; Chen, L.; Bao, X. Recent Developments in Micro-Structured Fiber Optic Sensors. *Fibers* 2017, *5*, 3. https://doi.org/10.3390/fib5010003.
76. Getinet Woyessa, Andrea Fasano, Christos Markos, Alessio Stefani, Henrik K. Rasmussen, and Ole Bang, "Zeonex microstructured polymer optical fiber: fabrication friendly fibers for high temperature and humidity insensitive Bragg grating sensing," Opt. Mater. Express 7, 286-295 (2017).
77. Yang, C.X.; Lu, Y.; Liu, L.B.; Yao, J. Fiber ring laser temperature sensor based on liquid-filled photonic crystal fiber. *J. Sci. IEEE Sens. J.* 2017, *99*, 6948–6952.
78. Wang, Y.; Huang, Q.; Zhu, W.; Yang, M.; Lewis, E. Novel optical fiber SPR temperature sensor based on MMF-PCF-MMF structure and gold-PDMS film. *J. Sci. Opt. Express* 2018, *26*, 1910.
79. Gao, H.; Hu, H.; Zhao, Y.; Li, J.; Lei, M.; Zhang, Y. Highly-sensitive optical fiber temperature sensors based on PDMS/silica hybrid fiber structures. *Sens. Actuators A Phys.* 2018, *284*, 22–27.
80. Sanzhar Korganbayev, Rui Min, Madina Jelbuldina, Xuehao Hu, Christophe Caucheteur, Ole Bang, Beatriz Ortega, Carlos Marques, and Daniele Tosi, "Thermal Profile Detection Through High-Sensitivity Fiber Optic Chirped Bragg Grating on Microstructured PMMA Fiber," J. Lightwave Technol. 36, 4723-4729 (2018).
81. Yong Zhao, Qi-lu Wu, Ya-nan Zhang, "Theoretical analysis of high-sensitive seawater temperature and salinity measurement based on C-type micro-structured fiber", Sensors and Actuators B: Chemical, 258, 822-828, 2018, https://doi.org/10.1016/j.snb.2017.11.179.
82. A. Lopez-Aldaba, J. -L. Auguste, R. Jamier, P. Roy and M. López-Amo, "Simultaneous Strain and Temperature Multipoint Sensor Based on Microstructured Optical Fiber," in *Journal of Lightwave Technology*, 36(4), 910-916, 2018, doi: 10.1109/JLT.2017.2752278.
83. Ying-gang Liu, Xin Liu, Cheng-ju Ma, Yu-min Zhou, "Micro-structured optical fiber sensor for simultaneous measurement of temperature and refractive index," Optical Fiber Technology, 41, 168-172, 2018, https://doi.org/10.1016/j.yofte.2018.01.019.
84. Lei Zhao, Haixia Han, Yudong Lian, Nannan Luan, Jianfei Liu, "Theoretical analysis of all-solid D-type photonic crystal fiber based plasmonic sensor for refractive index and temperature sensing," Optical Fiber Technology, 50, 165-171, 2019, https://doi.org/10.1016/j.yofte.2019.03.013.
85. Huaiyin Su, Yundong Zhang, Kai Ma, Yongpeng Zhao, and Jinfang Wang, "High-temperature sensor based on suspended-core microstructured optical fiber," Optics Express, 27(15), 20156-20164, 2019.
86. L. Zhao, Y. Zhang, Y. Chen, and J. Wang, "Composite cavity fiber tip Fabry-Perot interferometer for high temperature sensing," Opt. Fiber Technol. 50, 31–35 (2019).
87. Mingjian Ma, Hailiang Chen, Wenxun Zhang, Shuguang Li and Xili Jing, "Temperature sensor based on a Sagnac interferometer using a liquid crystal-filled microstructured optical fiber," Mater. Res. Express **6** 085205, 2019.
88. Jincheng Zhao, Yong Zhao, Lu Bai, Ya-nan Zhang, "Sagnac Interferometer Temperature Sensor Based on Microstructured Optical Fiber Filled with Glycerin," Sensors and Actuators A: Physical, 314, 112245-7, 2020, https://doi.org/10.1016/j.sna.2020.112245.
89. Abdullah, H., Mitu, S.A. & Ahmed, K. Magnetic Fluid-Injected Ring-Core-Based Micro-structured Optical Fiber for Temperature Sensing in Broad Wavelength Spectrum. J. Electron. Mater. **49**, 4969–4976 (2020). https://doi.org/10.1007/s11664-020-08231-6.
90. Mingyue Wang, Hailiang Chen, Xili Jing, Shuguang Li, Mingjian Ma, Wenxun Zhang, Yingyue Zhang, "Temperature sensor based on modes coupling effect in a liquid crystal-filled microstructured optical fiber," Optik, 219, 165044-9, 2020, https://doi.org/10.1016/j.ijleo.2020.165044.
91. Baoluo Zheng, Jing Yang, Fuxin Qi, Jinhang Wang, Xin Zhang, Pu Wang, "Fabrication of Yb-doped silica micro-structured optical fibers from UV-curable nano-composites and their application in temperature sensing," Journal of Non-Crystalline Solids, 573, 121129-8, 2021, https://doi.org/10.1016/j.jnoncrysol.2021.121129.
92. Hongyu Li, Shuguang Li, Shun Wang, Song Zhang, "Theoretical analysis of a microstructured fiber temperature sensor based on a Sagnac interferometer with a wide temperature measurement range," Photonics and Nanostructures - Fundamentals and Applications, 43, 100858, 2021, https://doi.org/10.1016/j.photonics.2020.100858.
93. Li, S.; Zhang, S.; Guo, Y.; Li, H.; Wang, Y.; Zhou, X.; Cheng, T. Experiment and Analysis of Temperature Sensing of Microstructured Fiber with Silver and PDMS Films. *Sensors* **2022**, *22*, 1447. https://doi.org/10.3390/s22041447
94. Xiaoyu Chen, Xin Yan, Xuenan Zhang, Fang Wang, Takenobu Suzuki, Yasutake Ohishi, Tonglei Cheng, "Highly sensitive nonlinear temperature sensor based on soliton self-frequency shift technique in a

microstructured optical fiber," Sensors and Actuators A: Physical, 334, 113333, 2022, https://doi.org/10.1016/j.sna.2021.113333.

95. Ying Liang, Hao Zhang, Bangcai Huang, Bo Liu, Wei Lin, Jianjun Sun, Dongbo Wang, "Ultrahigh-sensitivity temperature sensor based on resonance coupling in liquid-infiltrated side-hole microstructured optical fibers," Sensors and Actuators A: Physical, 334, 113358, 2022, https://doi.org/10.1016/j.sna.2021.113358.
96. Xian Zhang, Yangyang Xu, Xiao-Song Zhu, and Yi-Wei Shi, "Surface plasmon resonance temperature sensor with tunable detection range based on a silver-coated multi-hole optical fiber," Opt. Express 30, 48091-48102, 2022.
97. W. Wildner and D. Drummer, "A Fiber Optic Temperature Sensor Based on the Combination of Two Materials With Different Thermo-Optic Coefficients," in IEEE Sensors Journal, vol. 16, no. 3, pp. 688-692, Feb.1, 2016.
98. Kun Wang et al, "Temperature sensing based on multimode interference in polymer optical fibers: sensitivity enhancement by PC-APC connections", Jpn. J. Appl. Phys. 61 118001, 2022.
99. Xiaoyan Sun, Limu Zhang, Li Zeng, Youwang Hu, Ji-an Duan, "Micro-bending sensing based on single-mode fiber spliced multimode fiber Bragg grating structure", Optics Communications, Volume 505, 127513, 2022.
100. Zhan Wang, DeLi Chen, XianChao Yang, SiXiang Liang, XiaoHong Sun, "Temperature sensor of single-mode-no-core-single-mode fiber structure coated with PDMS", Optical Fiber Technology, Volume 68, 102793, 2022.
101. Xiaowei Li, Jianchang Tan, Wei Li, Chao Yang, Qilong Tan, Guoying Feng, "A high-sensitivity optical fiber temperature sensor with composite materials", Optical Fiber Technology, Volume 68, 102821, 2022.
102. Q. Huang et al., "Graphene–Gold–Au@Ag NPs-PDMS Films Coated Fiber Optic for Refractive Index and Temperature Sensing," in IEEE Photonics Technology Letters, vol. 31, no. 15, pp. 1205-1208, 2019.
103. Han Gao, Haifeng Hu, Yong Zhao, Jin Li, Ming Lei, Yong Zhang, "Highly-sensitive optical fiber temperature sensors based on PDMS/silica hybrid fiber structures", Sensors and Actuators A: Physical, Volume 284, 22-27, 2018.
104. Lu Cai, Yin Liu, Sheng Hu, Qiang Liu, "Optical fiber temperature sensor based on modal interference in multimode fiber lengthened by a short segment of polydimethylsiloxane", Microwave and Optical Technology Letters, vol. 61,6, 1656-1660, 2019.
105. Xingling Peng, Yingpeng Cha, Hua Zhang, Yulong Li, Jianxiong Ye, "Light intensity modulation temperature sensor based on U-shaped bent single-mode fiber", Optik, vol.130, 813-817, 2017.
106. W. Wildner and D. Drummer, "A Fiber Optic Temperature Sensor Based on the Combination of Two Materials With Different Thermo-Optic Coefficients," in IEEE Sensors Journal, vol. 16, no. 3, pp. 688-692, Feb.1, 2016.
107. M. Y. Mohd Noor et al., "High Sensitivity of Balloon-Like Bent MMI Fiber Low-Temperature Sensor," in IEEE Photonics Technology Letters, vol. 27, no. 18, pp. 1989-1992, 15 Sept.15, 2015.
108. Xia Hao, Zhengrong Tong, Weihua Zhang, Ye Cao, "A fiber laser temperature sensor based on SMF core-offset structure", Optics Communications, Vol. 335, 78-81, 2015.
109. Manoj Kumar, Arun Kumar, Saurabh Mani Tripathi, "A comparison of temperature sensing characteristics of SMS structures using step and graded index multimode fibers", Optics Communications, Vol. 312, 222-226, 2014.
110. R. Yang et al., "A Highly Sensitive Temperature Sensor Based on a Liquid-Sealed S-Tapered Fiber," in IEEE Photonics Technology Letters, vol. 25, no. 9, pp. 829-832, 2013.
111. Tan X, Geng Y, Li X, Gao R, Yin Z. High temperature microstructured fiber sensor based on a partial-reflection-enabled intrinsic Fabry-Perot interferometer. Appl Opt. 2013.
112. A. K. Mallik, A. Kumar, G. Gupta and A. Bhatnagar, "Single mode fiber-optic temperature sensor fabricated using wet etching," 2012 International Conference on Fiber Optics and Photonics (PHOTONICS), 2012, pp. 1-3.
113. Z. Cao, Z. Zhang, X. Ji, T. Shui, R. Wang, C. Yin, S. Zhen, L. Lu, B. Yu, "Strain insensitive and high temperature fiber sensor based on a Mach-Zehnder modal interferometer", Opt Fiber Technol. 20, 24–27, 2014.
114. A. Leal-Junior, A. Frizera-Netoc, C. Marques, M.J. Pontes, "A polymer optical fiber temperature sensor based on material features", SENSORS-BASEL. 18, 301, 2018.
115. A. Leal-Junior, J. Casas, C. Marques, M.J. Pontes, A. Frizera, "Application of additive layer manufacturing technique on the development of high sensitive fiber bragg grating temperature sensors", SENSORS-BASEL. 18, 4120, 2018.
116. Chiavaioli, F.; Gouveia, C.; Jorge, P.; Baldini, F. Towards a Uniform Metrological Assessment of Grating-Based Optical Fiber Sensors: From Refractometers to Biosensors. *Biosensors* **2017**, *7*, 23, doi:10.3390/bios7020023.

117. Hill, K. O.; Fujii, Y.; Johnson, D. C.; Kawasaki, B. S. Photosensitivity in optical fiber waveguides: Application to reflection filter fabrication. *Appl. Phys. Lett.* **1978**, *32*, 647–649, doi:10.1063/1.89881.
118. Rahman, B. M. A.; Viphavakit, C.; Chitaree, R.; Ghosh, S.; Pathak, A. K.; Verma, S.; Sakda, N. Optical Fiber, Nanomaterial, and THz-Metasurface-Mediated Nano-Biosensors: A Review. *Biosensors* **2022**, *12*, 42, doi:10.3390/bios12010042.
119. Zaynetdinov, M.; See, E. M.; Geist, B.; Ciovati, G.; Robinson, H. D.; Kochergin, V. A Fiber Bragg Grating Temperature Sensor for 2–400 K. *IEEE Sens. J.* **2015**, *15*, 1908–1912, doi:10.1109/JSEN.2014.2368457.
120. Hsiao, T.-C.; Hsieh, T.-S.; Chen, Y.-C.; Huang, S.-C.; Chiang, C.-C. Metal-coated fiber Bragg grating for dynamic temperature sensor. *Optik (Stuttg).* **2016**, *127*, 10740–10745, doi:10.1016/j.ijleo.2016.08.110.
121. Dong, N.; Wang, S.; Jiang, L.; Jiang, Y.; Wang, P.; Zhang, L. Pressure and Temperature Sensor Based on Graphene Diaphragm and Fiber Bragg Gratings. *IEEE Photonics Technol. Lett.* **2018**, *30*, 431–434, doi:10.1109/LPT.2017.2786292.
122. Jasmi, F.; Azeman, N. H.; Bakar, A. A. A.; Zan, M. S. D.; Haji Badri, K.; Su'ait, M. S. Ionic Conductive Polyurethane-Graphene Nanocomposite for Performance Enhancement of Optical Fiber Bragg Grating Temperature Sensor. *IEEE Access* **2018**, *6*, 47355–47363, doi:10.1109/ACCESS.2018.2867220.
123. Cheng, P.; Wang, L.; Pan, Y.; Yan, H.; Gao, D.; Wang, J.; Zhang, H. Fiber Bragg grating temperature sensor of cladding with SrTiO 3 thin film by pulsed laser deposition. *Laser Phys.* **2019**, *29*, 025107, doi:10.1088/1555-6611/aaf635.
124. Gao, X.; Ning, T.; Zhang, C.; Xu, J.; Zheng, J.; Lin, H.; Li, J.; Pei, L.; You, H. A dual-parameter fiber sensor based on few-mode fiber and fiber Bragg grating for strain and temperature sensing. *Opt. Commun.* **2020**, *454*, 124441, doi:10.1016/j.optcom.2019.124441.
125. Chen, Q.; Wang, D. N.; Gao, F. Simultaneous refractive index and temperature sensing based on a fiber surface waveguide and fiber Bragg gratings. *Opt. Lett.* **2021**, *46*, 1209, doi:10.1364/OL.419636.
126. Esposito, F.; Campopiano, S.; Iadicicco, A. Miniaturized Strain-Free Fiber Bragg Grating Temperature Sensors. *IEEE Sens. J.* **2022**, *22*, 16898–16903, doi:10.1109/JSEN.2022.3192355.
127. Fu, H.; Wang, S.; Chang, H.; You, Y. A high resolution and large range fiber Bragg grating temperature sensor with vortex beams. *Opt. Fiber Technol.* **2020**, *60*, 102369, doi:10.1016/j.yofte.2020.102369.
128. Li, G.; Ji, L.; Li, G.; Su, J.; Wu, C. High-resolution and large-dynamic-range temperature sensor using fiber Bragg grating Fabry-Pérot cavity. *Opt. Express* **2021**, *29*, 18523, doi:10.1364/OE.426398.
129. He, J.; Xu, X.; Du, B.; Xu, B.; Chen, R.; Wang, Y.; Liao, C.; Guo, J.; Wang, Y.; He, J. Stabilized Ultra-High-Temperature Sensors Based on Inert Gas-Sealed Sapphire Fiber Bragg Gratings. *ACS Appl. Mater. Interfaces* **2022**, *14*, 12359–12366, doi:10.1021/acsami.1c24589.
130. Guo, Q.; Zhang, Z.-D.; Zheng, Z.-M.; Pan, X.-P.; Chen, C.; Tian, Z.-N.; Chen, Q.-D.; Yu, Y.-S.; Sun, H.-B. Parallel-Integrated Sapphire Fiber Bragg Gratings Probe Sensor for High Temperature Sensing. *IEEE Sens. J.* **2022**, *22*, 5703–5708, doi:10.1109/JSEN.2022.3149508.
131. Xu, B.; He, J.; Du, B.; Xiao, X.; Xu, X.; Fu, C.; He, J.; Liao, C.; Wang, Y. Femtosecond laser point-by-point inscription of an ultra-weak fiber Bragg grating array for distributed high-temperature sensing. *Opt. Express* **2021**, *29*, 32615, doi:10.1364/OE.437479.
132. Sun, X.; Chang, Z.; Zeng, L.; Zhang, L.; Hu, Y.; Duan, J. Simultaneous vector bending and temperature sensing based on eccentric multi-mode fiber Bragg gratings. *Sensors Actuators A Phys.* **2021**, *331*, 112903, doi:10.1016/j.sna.2021.112903.
133. Hsu, C.-Y.; Chiang, C.-C.; Hsieh, T.-S.; Hsu, H.-C.; Tsai, L.; Hou, C.-H. Study of fiber Bragg gratings with TiN-coated for cryogenic temperature measurement. *Opt. Laser Technol.* **2021**, *136*, 106768, doi:10.1016/j.optlastec.2020.106768.
134. Ayupova, T.; Shaimerdenova, M.; Tosi, D. Shallow-Tapered Chirped Fiber Bragg Grating Sensors for Dual Refractive Index and Temperature Sensing. *Sensors* **2021**, *21*, 3635, doi:10.3390/s21113635.
135. Wang, Y.; Tao, J.; Yuan, W.; Lian, Z.; Ling, Q.; Chen, D.; Yu, Z.; Lu, C. Hollow Core Bragg Fiber Integrated With Regenerate Fiber Bragg Grating for Simultaneous High Temperature and gas Pressure Sensing. *J. Light. Technol.* **2021**, *39*, 5643–5649, doi:10.1109/JLT.2021.3088530.
136. Wang, H.; Gao, S.; Yue, X.; Cheng, X.; Liu, Q.; Min, R.; Qu, H.; Hu, X. Humidity-Sensitive PMMA Fiber Bragg Grating Sensor Probe for Soil Temperature and Moisture Measurement Based on Its Intrinsic Water Affinity. *Sensors* **2021**, *21*, 6946, doi:10.3390/s21216946.

137. Zhu, F.; Hao, X.; Zhang, Y.; Jia, P.; Su, J.; Wang, L.; Liu, L.; Li, X.; An, G. D-shaped optic fiber temperature and refractive index sensor assisted by tilted fiber bragg grating and PDMS film. *Sensors Actuators A Phys.* **2022**, *346*, 113870, doi:10.1016/j.sna.2022.113870.
138. Li, M.; Gong, Y.; Yin, J.; Li, W.; Shao, Y.; Cong, A.; Huang, G. Highly-sensitive and wide-range temperature sensor based on polymer-filled micro-cavity in fibre Bragg grating by temperature segmentation. *Optik (Stuttg).* **2021**, *245*, 167707, doi:10.1016/j.ijleo.2021.167707.